Nonlinear Dynamics

Andy Wolski

The Cockcroft Institute, and the University of Liverpool, UK

CAS: Introduction to Accelerator Physics
Prague, Czech Republic
September 2014

In this lecture, we shall discuss nonlinear dynamics in the context of two types of accelerator system:

1. a bunch compressor (a single-pass system);
2. a storage ring (a multi-turn system).

We shall use these examples to introduce a number of topics:

- Mathematical tools for modelling nonlinear dynamics:
  – *Taylor maps; symplectic maps.*
- Basic effects of nonlinear perturbations:
  – *resonances; tune shift with amplitude.*
- Analysis methods:
  – *normal form analysis; frequency map analysis.*
- Practical consequences of nonlinearities:
  – *phase space distortion; dynamic aperture.*

Our aim is to provide an introduction to some of the key concepts of nonlinear dynamics in particle accelerators.

By the end of the lecture, you should be able to:

- explain the significance and potential impact of nonlinear dynamics in some accelerator systems;
- outline some of the tools used for modelling nonlinear dynamics in accelerators;
- explain the importance of *symplectic maps*, and outline some of the challenges in their calculation and application;
- describe some of the features of nonlinear oscillators, and outline some of the analysis methods that can be used to characterise their behaviour.

As a first example, we discuss nonlinear longitudinal dynamics in a bunch compressor.

A bunch compressor reduces the length of a bunch, by performing a rotation in longitudinal phase space. Bunch compressors are used, for example, in free electron lasers to increase the peak current.

We shall follow these steps in our analysis:

1. Outline of structure and operation of a bunch compressor.
2. Specification of parameters based on linear dynamics.
3. Analysis of linear and nonlinear effects.
4. Adjustment of parameters to compensate nonlinear effects.

Bunch compressor: structure and operation

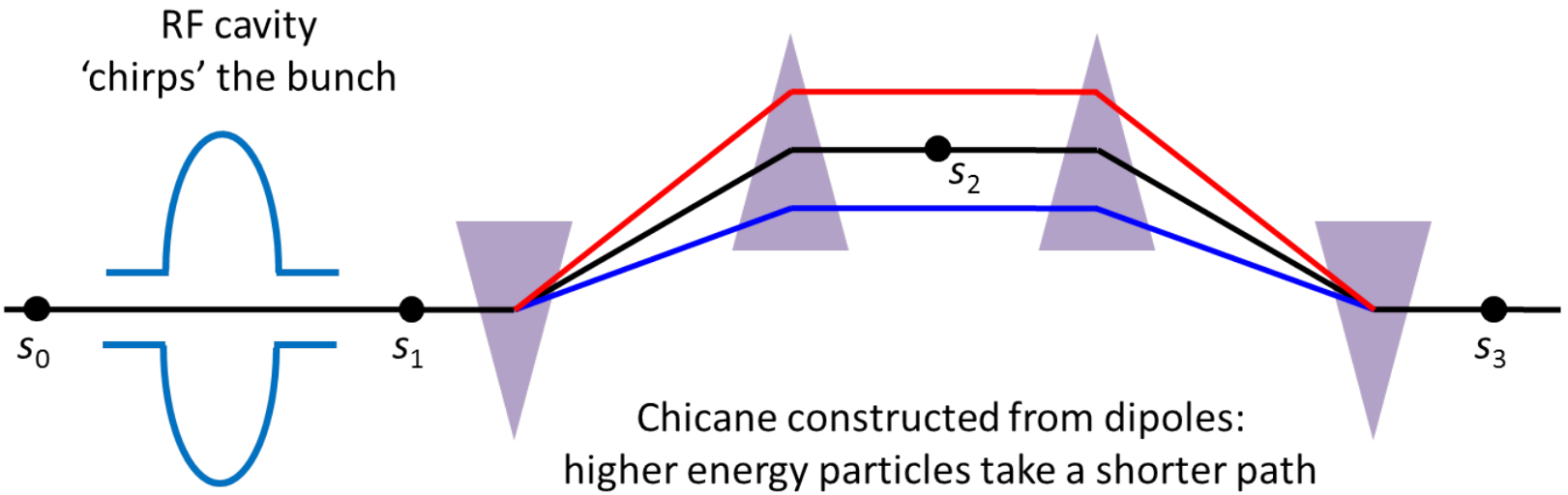

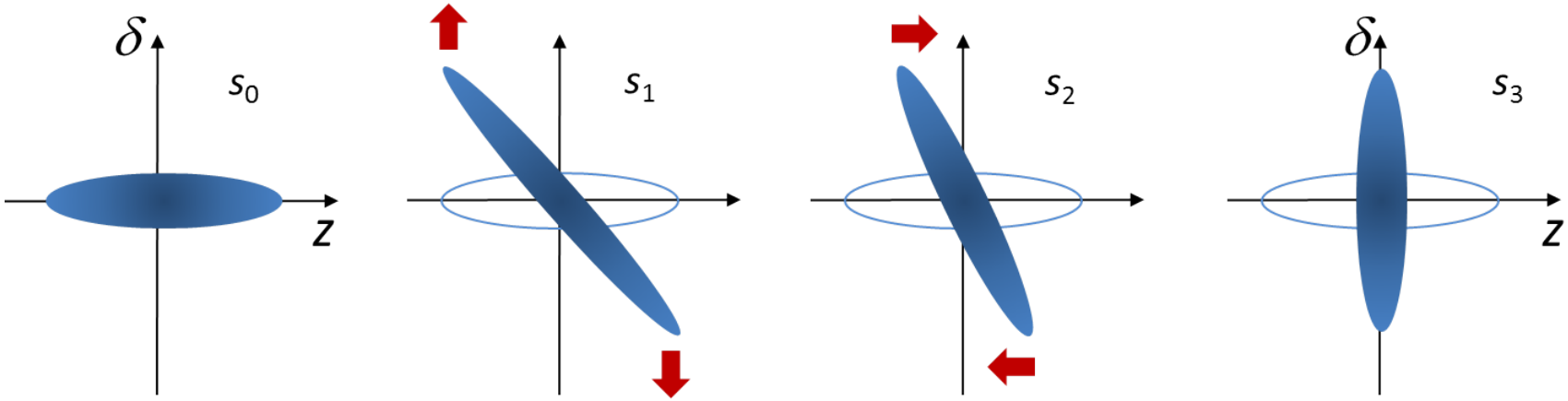

Distribution of particles 'rotates' in longitudinal phase space (area is conserved).

The rf cavity is designed to "chirp" the bunch, i.e. to provide a change in energy deviation as a function of longitudinal position z within the bunch ($z > 0$ at the head of the bunch).

The energy deviation δ of a particle with energy E is defined as:

$$\delta = \frac{E - E_0}{E_0}, \tag{1}$$

where E_0 is the reference energy for the system.

The transfer map for the rf cavity in the bunch compressor is:

$$z_1 = z_0, \tag{2}$$

$$\delta_1 = \delta_0 - \frac{eV}{E_0} \sin\left(\frac{\omega z_0}{c}\right), \tag{3}$$

where V is the rf voltage, and $\omega/2\pi$ is the rf frequency.

Neglecting synchrotron radiation, the chicane does not change the energy of the particles. However, the path length L depends on the energy of the particle.

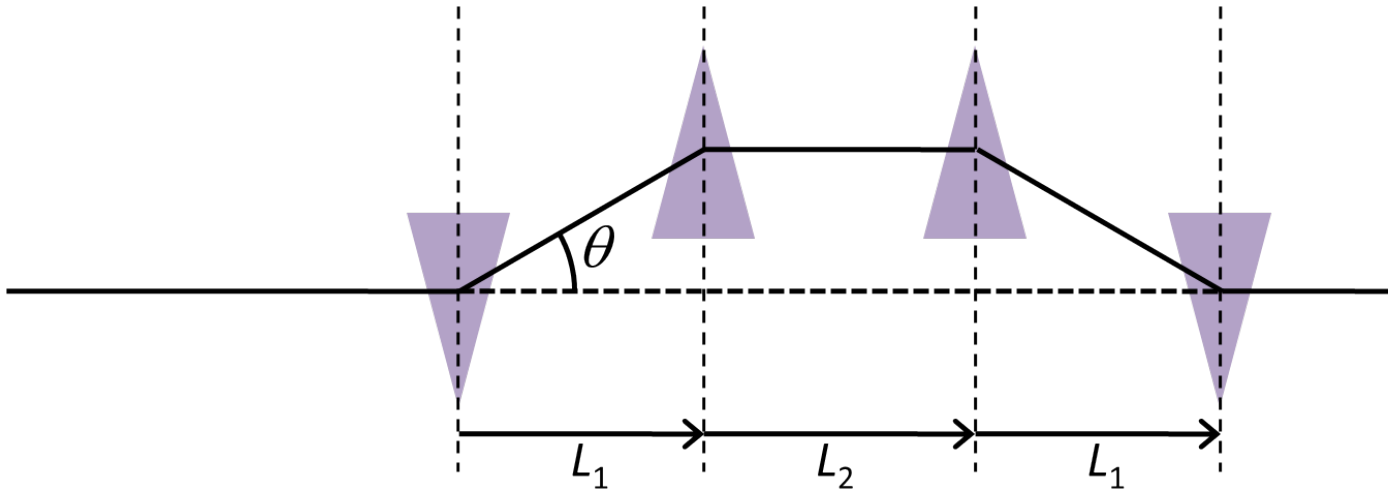

If we assume that the bending angle in a dipole is small, $\theta \ll 1$:

$$L = \frac{2L_1}{\cos\theta} + L_2. \tag{4}$$

The bending angle is a function of the energy of the particle:

$$\theta = \frac{\theta_0}{1+\delta}. \tag{5}$$

The change in the co-ordinate z is the difference between the nominal path length, and the length of the path actually taken by the particle.

Hence, the transfer map for the chicane can be written:

$$z_2 = z_1 + 2L_1 \left(\frac{1}{\cos\theta_0} - \frac{1}{\cos(\theta(\delta_1))} \right), \quad (6)$$

$$\delta_2 = \delta_1, \quad (7)$$

where θ_0 is the nominal bending angle of each dipole in the chicane, and $\theta(\delta)$ is given by (5):

$$\theta(\delta) = \frac{\theta_0}{1+\delta}.$$

Clearly, the complete transfer map for the bunch compressor is nonlinear; but how important are the nonlinear terms?

To understand the effects of the nonlinear part of the map, we shall look at a specific example.

First, we will "design" a bunch compressor using only the linear part of the map.

The linear part of a transfer map can be obtained by expanding the map as a Taylor series in the dynamical variables, and keeping only the first-order terms.

After finding appropriate values for the various parameters using the linear transfer map, we shall see how our design has to be modified to take account of the nonlinearities.

To first order in the dynamical variables z and δ, the map for the rf cavity can be written:

$$z_1 = z_0, \tag{8}$$
$$\delta_1 = \delta_0 + R_{65} z_0, \tag{9}$$

where:

$$R_{65} = -\frac{eV}{E_0}\frac{\omega}{c}. \tag{10}$$

The map for the chicane can be written:

$$z_2 = z_1 + R_{56}\delta_1, \tag{11}$$
$$\delta_2 = \delta_1, \tag{12}$$

where:

$$R_{56} = 2L_1\frac{\theta_0 \sin\theta_0}{\cos^2\theta_0}. \tag{13}$$

As a specific example, consider a bunch compressor for the International Linear Collider:

Initial rms bunch length	$\sqrt{\langle z_0^2 \rangle}$	6 mm
Initial rms energy spread	$\sqrt{\langle \delta_0^2 \rangle}$	0.15%
Final rms bunch length	$\sqrt{\langle z_2^2 \rangle}$	0.3 mm

Two constraints determine the values of R_{65} and R_{56}:

- The bunch length should be reduced by a factor 20.
- There should be no "chirp" on the bunch at the exit of the bunch compressor, i.e. $\langle z_2 \delta_2 \rangle = 0$.

With these constraints, we find (see Appendix A):

$$R_{65} = -4.9937\,\mathrm{m}^{-1}, \quad \text{and} \quad R_{56} = 0.19975\,\mathrm{m}. \tag{14}$$

We can illustrate the effect of the linearised bunch compressor map on phase space using an artificial "window frame" distribution:

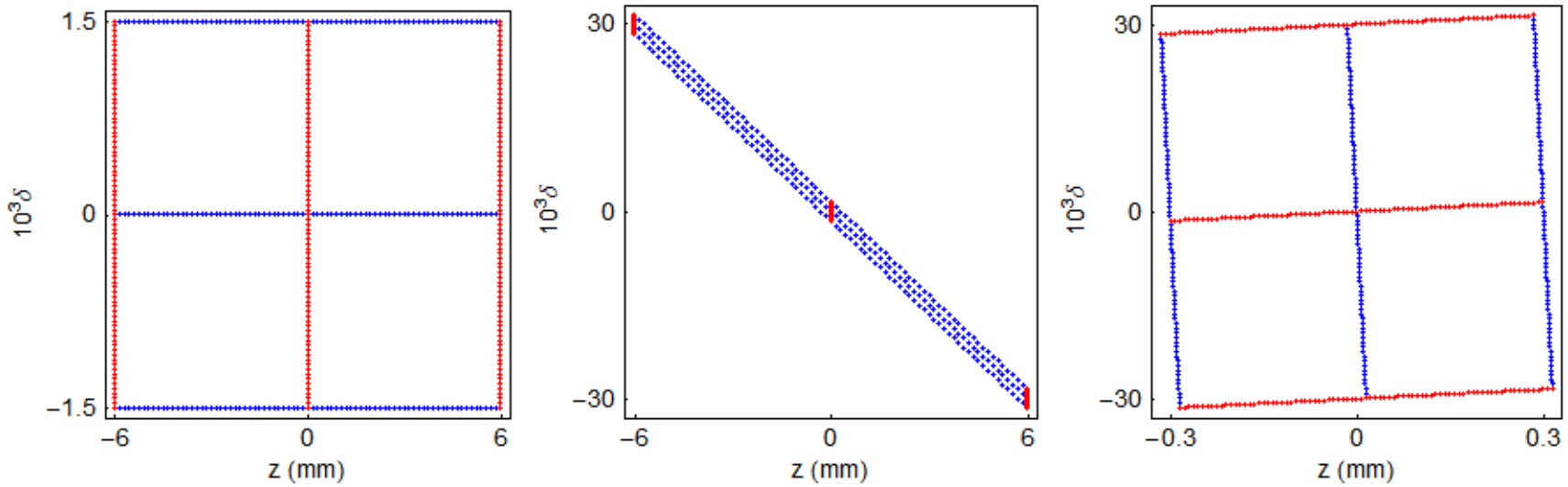

The rms bunch length is reduced by a factor of 20 as required, but the rms energy spread is *increased* by the same factor. This is because the transfer map is *symplectic*, so phase space areas are conserved under the transformation.

Now let us see what happens when we apply the full nonlinear map for the bunch compressor.

The full map cannot simply be represented by the two coefficients R_{65} and R_{56}: we need to make some assumptions for the rf voltage and frequency, and the dipole bending angle and chicane length.

We have to choose all these parameters so that the "linear" parameters have the appropriate values.

Beam (reference) energy	E_0	5 GeV
RF frequency	f_{rf}	1.3 GHz
RF voltage	V_{rf}	916 MV
Dipole bending angle	θ_0	3°
Dipole spacing	L_1	36.3 m

As before, we illustrate the effect of the bunch compressor map on phase space using a "window frame" distribution:

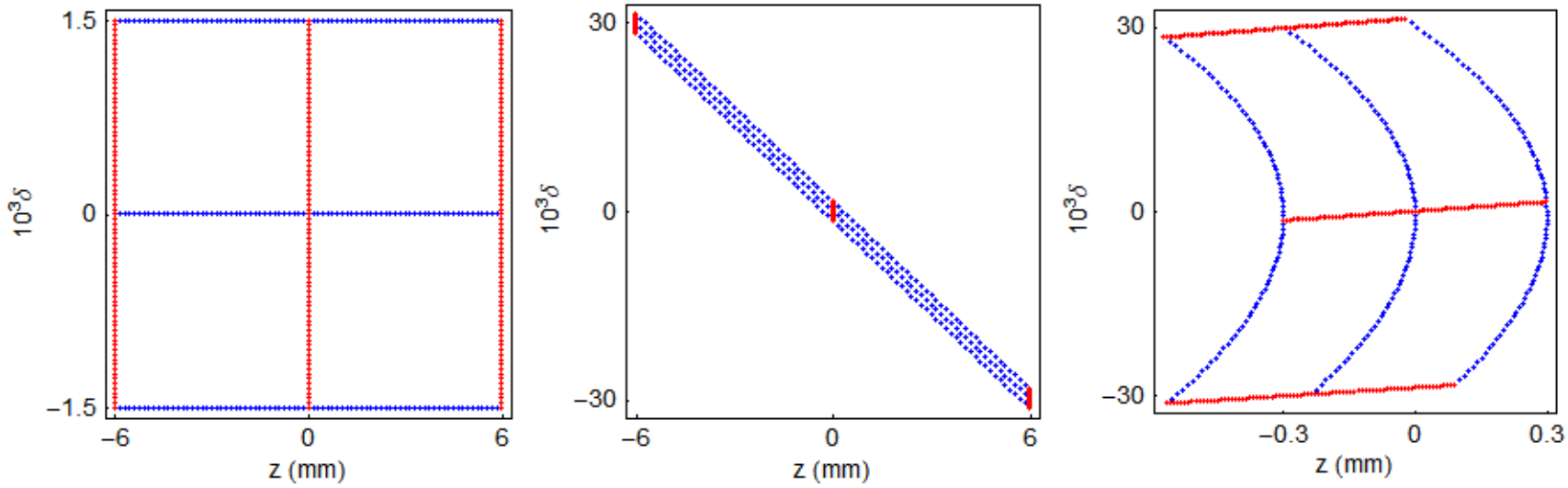

Although the bunch length has been reduced, there is significant distortion of the distribution: the rms bunch length will be significantly longer than we are aiming for.

To reduce the distortion, we first need to understand where it comes from, which means looking at the map more closely.

Consider a particle entering the bunch compressor with initial phase space co-ordinates z_0 and δ_0. We can write the co-ordinates z_1 and δ_1 of the particle after the rf cavity *to second order* in z_0 and δ_0:

$$z_1 = z_0, \tag{15}$$

$$\delta_1 = \delta_0 + R_{65} z_0 + T_{655} z_0^2. \tag{16}$$

Note the notation for the coefficients in the map: the first subscript indicates the variable on the left hand side of the equation, and subsequent subscripts indicate the variables in the relevant term.

By convention, R is used for the coefficients of linear terms, T for second-order terms, U for third-order terms, and so on.

The co-ordinates of the particle after the chicane are then (to second order):

$$z_2 = z_1 + R_{56}\delta_1 + T_{566}\delta_1^2, \quad (17)$$

$$\delta_2 = \delta_1. \quad (18)$$

If we combine the maps for the rf and the chicane, we get:

$$\begin{aligned} z_2 = {} & (1 + R_{56}R_{65})z_0 + R_{56}\delta_0 \\ & + (R_{56}T_{655} + R_{65}^2 T_{566})z_0^2 \\ & + 2R_{65}T_{566}z_0\delta_0 \\ & + T_{566}\delta_0^2, \end{aligned} \quad (19)$$

$$\delta_2 = \delta_0 + R_{65}z_0 + T_{655}z_0^2. \quad (20)$$

The term that gives the strong nonlinear distortion is the term in z_0^2 in (19). If we can design a system such that the appropriate coefficients satisfy:

$$R_{56}T_{655} + R_{65}^2 T_{566} = 0, \tag{21}$$

then we should be able to reduce the distortion.

The values of R_{56} and R_{65} are determined by the required compression factor.

The value of T_{566} is determined by the chicane; by expanding (6) as a Taylor series in δ, we find for $\theta_0 \ll 1$:

$$T_{566} \approx -3L_1\theta_0^2. \tag{22}$$

That leaves us with T_{655}. This is the second-order dependence of the energy deviation on longitudinal position for a particle passing through the rf cavity. But if we inspect the full rf map (3), we find it contains only odd-order terms, unless...

...we operate the rf cavity off-phase. In other words, we have to modify the rf transfer map to:

$$z_1 = z_0, \tag{23}$$

$$\delta_1 = \delta_0 - \frac{eV}{E_0}\sin\left(\frac{\omega z_0}{c} + \phi_0\right). \tag{24}$$

The first-order coefficient in the transfer map for δ is then:

$$R_{65} = -\frac{eV}{E_0}\frac{\omega}{c}\cos\phi_0. \tag{25}$$

The second-order coefficient is:

$$T_{655} = \frac{1}{2}\frac{eV}{E_0}\left(\frac{\omega}{c}\right)^2\sin\phi_0. \tag{26}$$

Note that there is also a zeroth-order term, so the bunch ends up with a non-zero mean energy deviation $\langle\delta\rangle$ after the rf cavity; but we can take this into account simply by an appropriate scaling of the field in the chicane.

The linear coefficients are determined by the required compression factor, and the requirement to have zero final correlation $\langle z\delta \rangle$. For the ILC bunch compressor:

$$R_{65} = -4.9937\,\mathrm{m}^{-1}, \quad \text{and} \quad R_{56} = 0.19975\,\mathrm{m}. \tag{27}$$

The value of T_{566} is determined by the parameters of the chicane:

$$T_{566} \approx -3L_1\theta_0^2 = -0.29963\,\mathrm{m}. \tag{28}$$

And the value of T_{655} is determined by the need to correct the second-order distortion of the phase space:

$$R_{56}T_{655} + R_{65}^2 T_{566} = 0 \quad \therefore \quad T_{655} = 37.406\,\mathrm{m}^{-2}. \tag{29}$$

Now, given:

$$R_{65} = -\frac{eV}{E_0}\frac{\omega}{c}\cos\phi_0 = -4.9937\,\mathrm{m}^{-1}, \tag{30}$$

and:

$$T_{655} = \frac{1}{2}\frac{eV}{E_0}\left(\frac{\omega}{c}\right)^2\sin\phi_0 = 37.406\,\mathrm{m}^{-2}, \tag{31}$$

we find, for $E_0 = 5\,\mathrm{GeV}$ and $\omega = 1.3\,\mathrm{GHz}$:

$$V = 1,046\,\mathrm{MV}, \quad \text{and} \quad \phi_0 = 28.8^\circ. \tag{32}$$

Operating with this phase, we are providing over a gigavolt of rf to *decelerate* the beam by more than 500 MV.

Because of adiabatic (anti)damping, we will need to reduce the R_{56} of the chicane by a factor E_1/E_0, where E_0 and E_1 are the mean bunch energy before and after the rf, respectively.

Also, the phase space area occupied by the distribution will be increased by a factor E_0/E_1.

As before, we illustrate the effect of the bunch compressor on phase space using a "window frame" distribution. But now we use the parameters determined above, to try to compress by a factor 20, while minimising the second-order distortion:

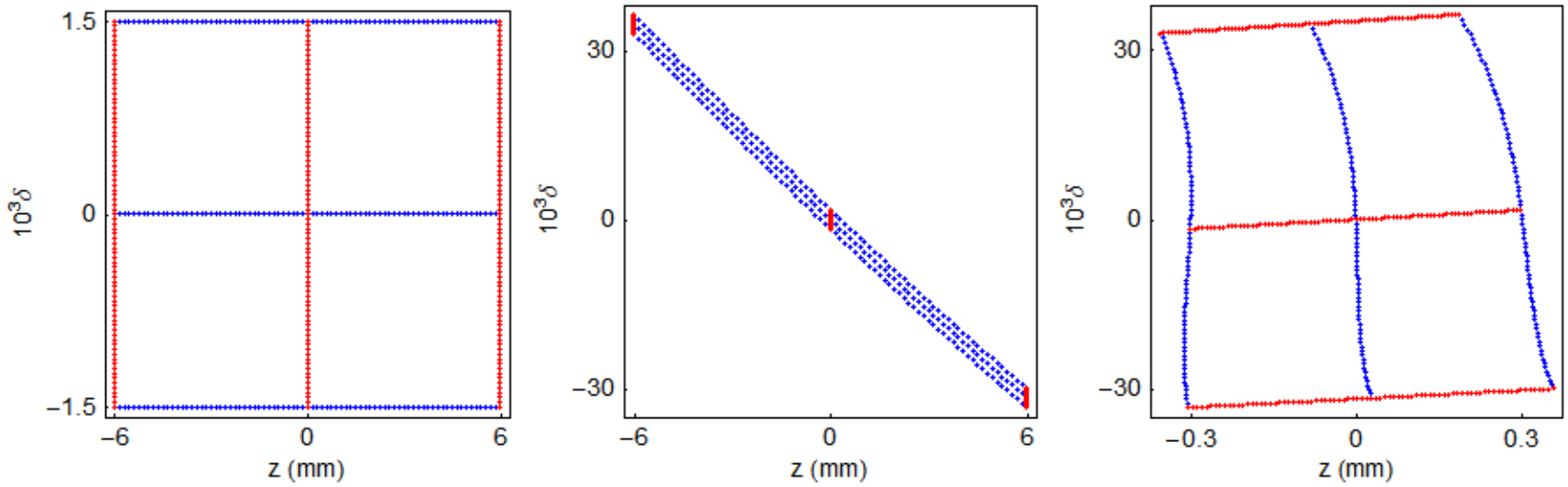

This looks much better: the dominant distortion now appears to be third-order, and looks small enough that it should not significantly affect the performance of the machine.

We have already learned some useful lessons from this example:

- Nonlinear effects can limit the performance of an accelerator system. Sometimes the effects can be ignored; however, in many cases, a system designed without taking account of nonlinearities will not achieve the specified performance.

- If we take the trouble to analyse and understand the nonlinear behaviour of a system, then, if we are fortunate enough and clever enough, we may be able to devise a means of compensating any adverse effects.

As a second example, let us consider the transverse dynamics in a simple storage ring. We shall assume that:

- The storage ring is constructed from some number of identical cells consisting of dipoles, quadrupoles and sextupoles.
- The phase advance per cell can be tuned from close to zero, up to about $0.5 \times 2\pi$.
- There is one sextupole per cell, which is located at a point where the horizontal beta function is 1 m, and the alpha function is zero.

Usually, storage rings will contain (at least) two sextupoles per cell, to correct horizontal and vertical chromaticity. To keep things simple, we will use only one sextupole per cell.

Sextupoles are needed in a storage ring to compensate for the fact that quadrupoles have lower focusing strength for particles of higher energy:

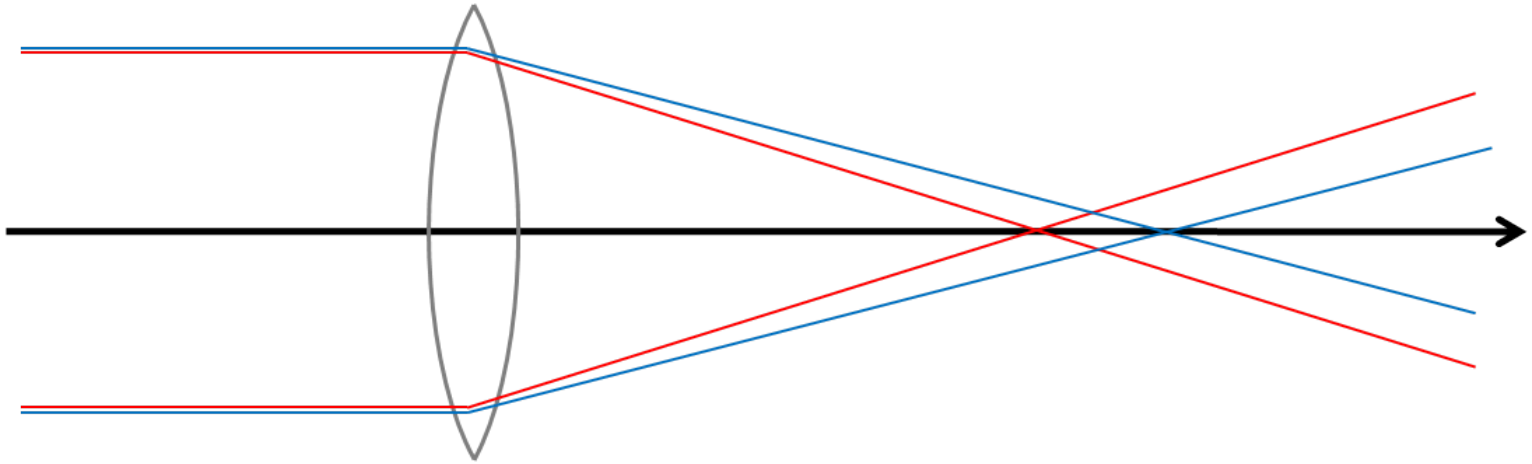

The change in focusing strength with particle energy has undesirable consequences, especially in storage rings: it can lead to particle motion becoming unstable because of resonances.

A sextupole can be regarded as a quadrupole with focusing strength that increases with horizontal offset from the axis.

If sextupoles are located where there is non-zero dispersion, they can be used to control the chromaticity in a storage ring.

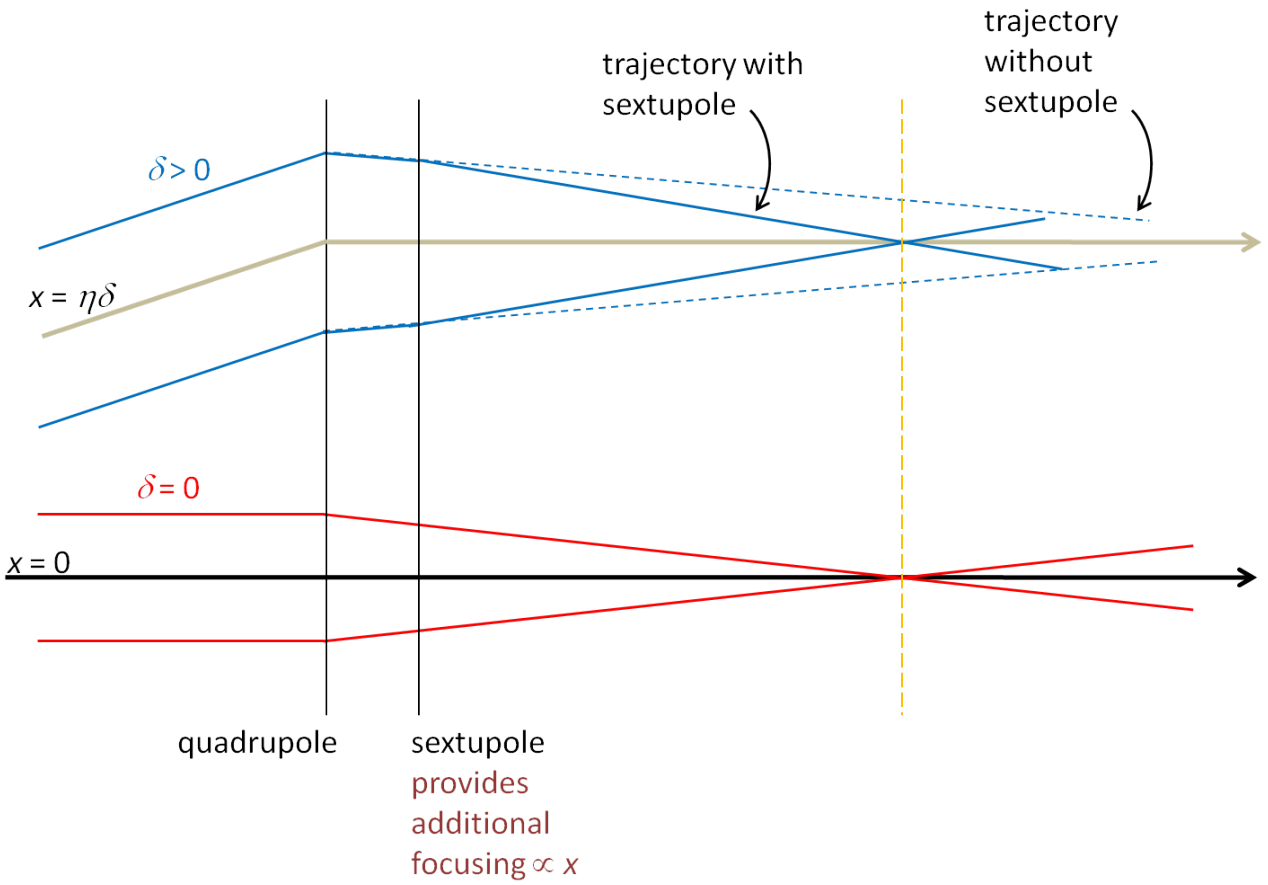

The chromaticity, and hence the sextupole strength, will normally be a function of the phase advance.

However, just to investigate the nonlinear effects of the sextupoles, we shall keep the sextupole strength $k_2 L$ fixed, and change only the phase advance.

We can assume that the map from one sextupole to the next is linear, and corresponds to a rotation in phase space through an angle equal to the phase advance:

$$\begin{pmatrix} x \\ p_x \end{pmatrix} \mapsto \begin{pmatrix} \cos\mu_x & \sin\mu_x \\ -\sin\mu_x & \cos\mu_x \end{pmatrix} \begin{pmatrix} x \\ p_x \end{pmatrix}. \tag{33}$$

Again to keep things simple, we shall consider only horizontal motion, and assume that the vertical coordinate $y = 0$.

The change in the horizontal momentum of a particle moving through the sextupole is found by integrating the Lorentz force:

$$\Delta p_x = -\int_0^L \frac{B_y}{B\rho}\, ds. \tag{34}$$

The sextupole strength k_2 is defined by:

$$k_2 = \frac{1}{B\rho}\frac{\partial^2 B_y}{\partial x^2}, \tag{35}$$

where $B\rho$ is the beam rigidity. For a pure sextupole field (assuming that the vertical coordinate $y = 0$),

$$\frac{B_y}{B\rho} = \frac{1}{2}k_2 x^2. \tag{36}$$

If the sextupole is short, then we can neglect the small change in the coordinate x as the particle moves through the sextupole, in which case:

$$\Delta p_x \approx -\frac{1}{2}k_2 L x^2. \tag{37}$$

The map for a particle moving through a short sextupole can be represented by a "kick" in the horizontal momentum:

$$x \mapsto x, \tag{38}$$

$$p_x \mapsto p_x - \frac{1}{2} k_2 L x^2. \tag{39}$$

Let us choose a fixed value $k_2 L = -600\,\mathrm{m}^{-2}$, and look at the effects of the maps for different phase advances.

For each case, we construct a *phase space portrait* by plotting the values of the dynamical variables after repeated application of the map (equation (33), followed by (38) and (39)) for a range of initial conditions.

First, let us look at the phase space portraits for a range of phase advances from $0.2 \times 2\pi$ to $0.5 \times 2\pi$.

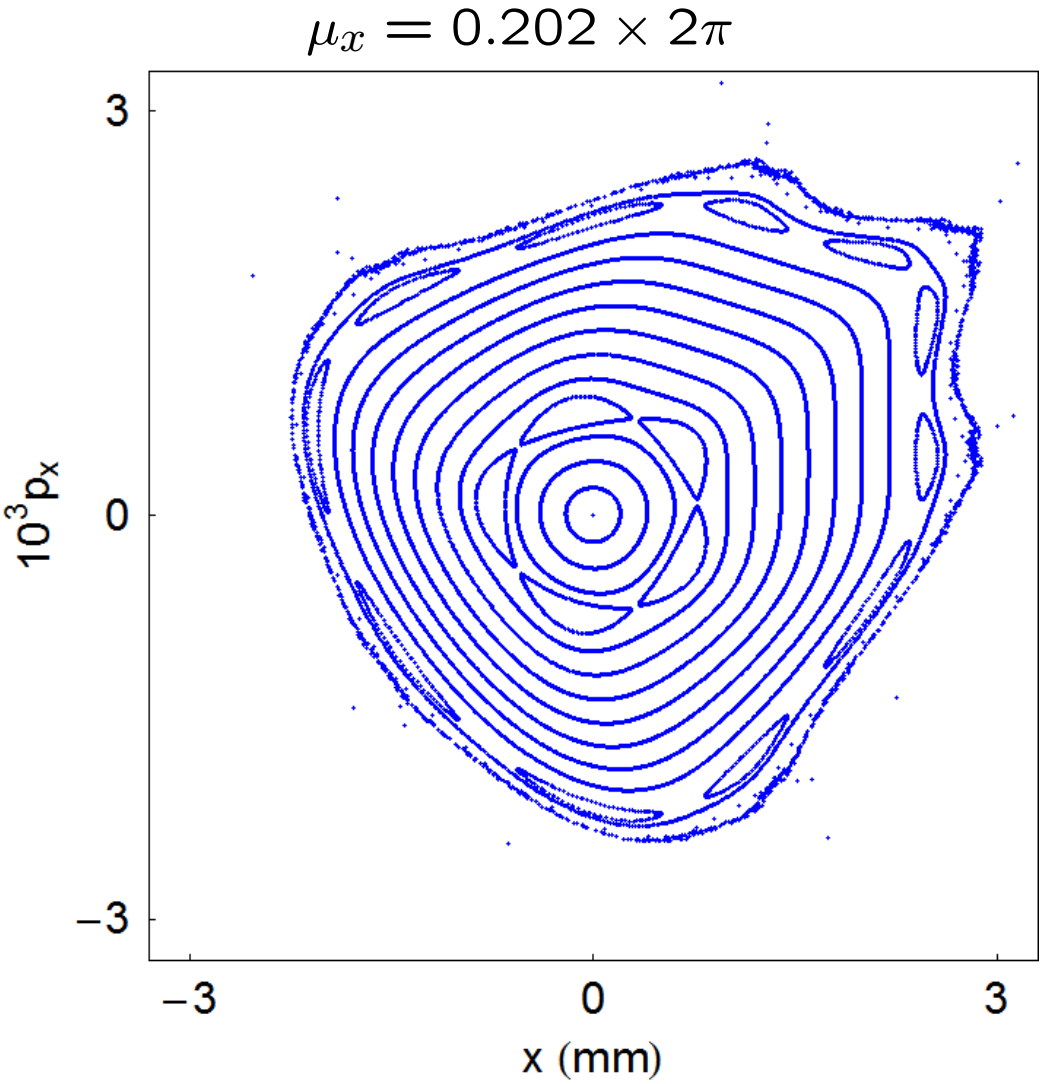
$\mu_x = 0.202 \times 2\pi$
3
0
−3
$10^3 p_x$
−3
0
3
x (mm)

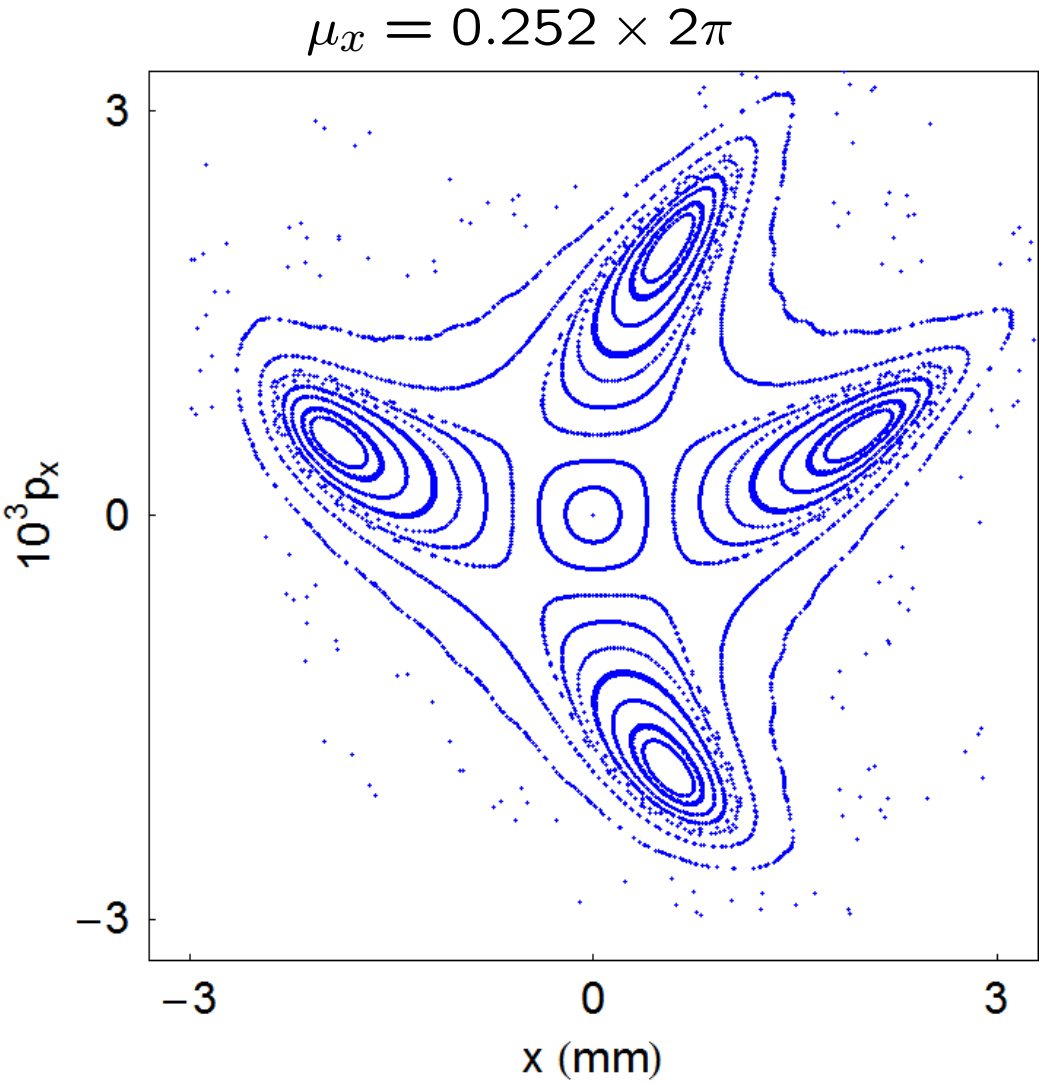
$\mu_x = 0.252 \times 2\pi$
3
0
−3
$10^3 p_x$
−3
0
3
x (mm)

Phase space portraits: storage ring with a single sextupole

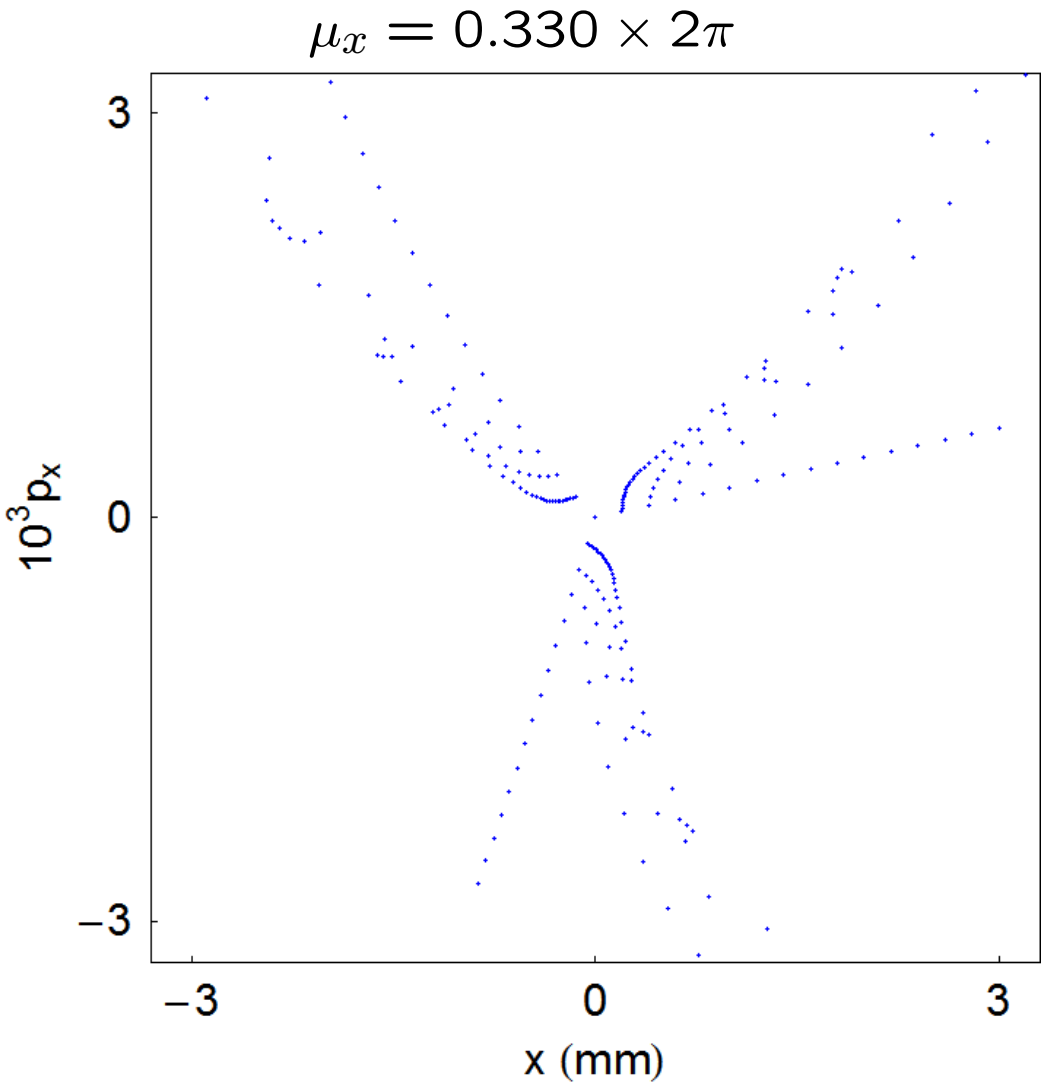

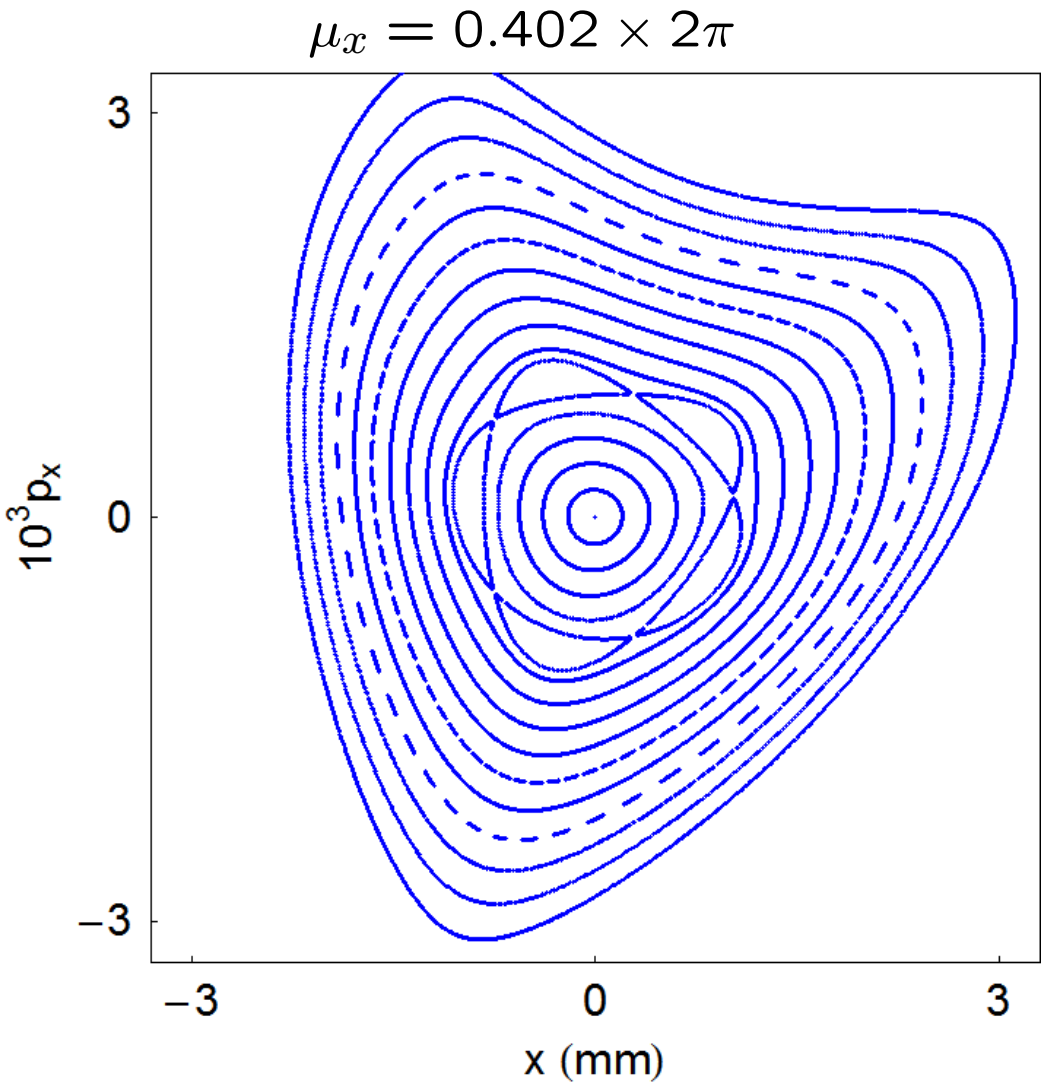
$\mu_x = 0.402 \times 2\pi$
3
0
−3
$10^3 p_x$
−3
0
3
x (mm)

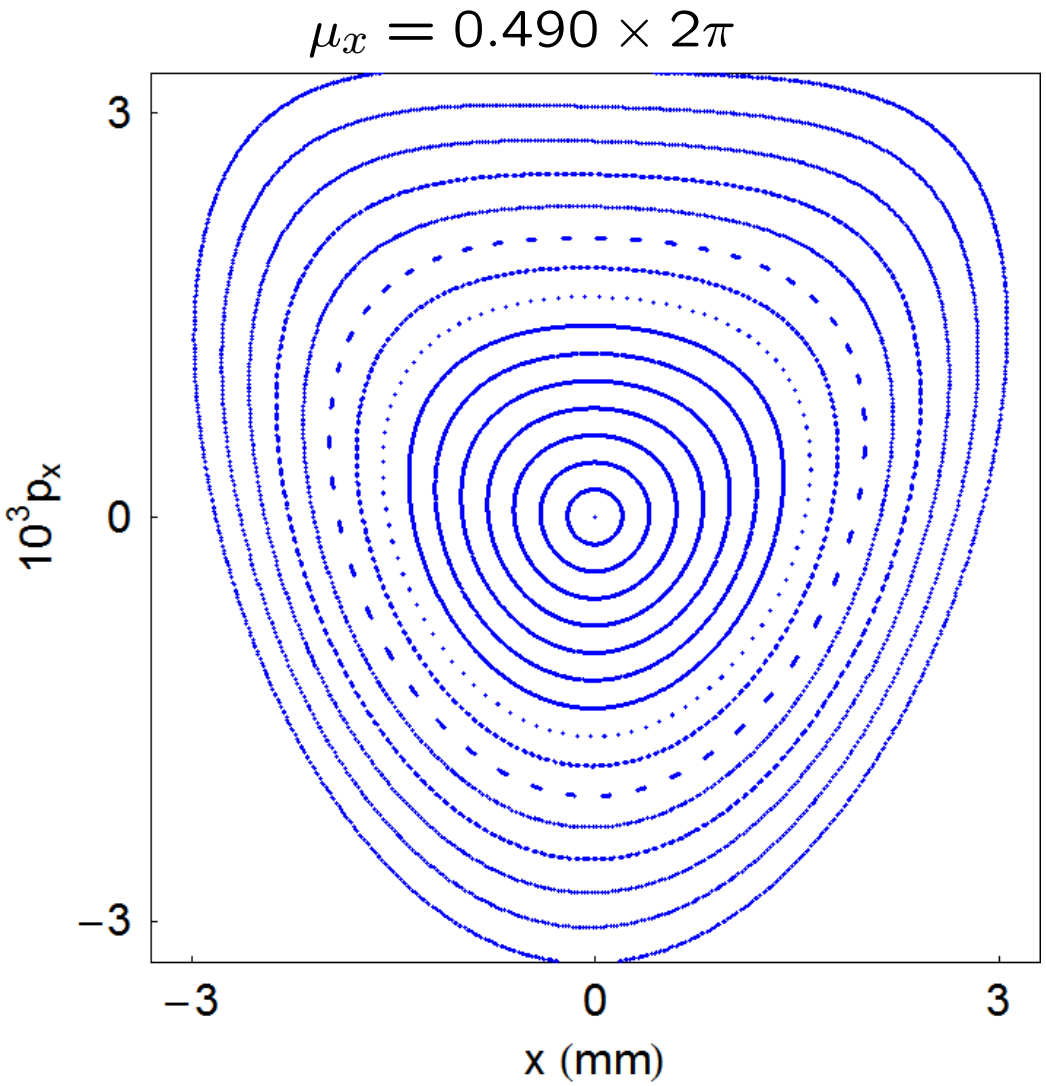
$\mu_x = 0.490 \times 2\pi$
3
0
−3
$10^3 p_x$
−3
0
3
x (mm)

There are some interesting features in these phase space portraits to which it is worth drawing attention:

- For small amplitudes (small x and p_x), particles trace out closed loops around the origin: this is what we expect for a purely linear map.
- As the amplitude is increased, there appear "islands" in phase space: the phase advance (for the linear map) is often close to m/p where m is an integer and p is the number of islands.
- Sometimes, a larger number of islands appears at larger amplitude.
- Usually, there is a closed curve that divides a region of stable motion from a region of unstable motion. Outside that curve, the amplitude of particles increases without limit as the map is repeatedly applied.
- The area of the stable region depends strongly on the phase advance: for a phase advance close to $2\pi/3$, it appears that the stable region almost vanishes altogether.
- It appears that as the phase advance is increased towards π, the stable area becomes large, and distortions from the linear ellipse become less evident.

An important observation is that the effect of the sextupole in the periodic cell depends strongly on the phase advance across the cell.

We can start to understand the significance of the phase advance by considering two special cases:

1. phase advance equal to an integer times 2π;
2. phase advance equal to a half integer times 2π.

Let us consider first what happens when the phase advance is an integer. In that case, the linear part of the map is just the identity:

$$x \mapsto x, \tag{40}$$

$$p_x \mapsto p_x. \tag{41}$$

So the combined effect of the linear map and the sextupole kick is:

$$x \mapsto x, \tag{42}$$

$$p_x \mapsto p_x - \frac{1}{2} k_2 L x^2. \tag{43}$$

Clearly, for $x \neq 0$, the horizontal momentum will increase without limit. There are no stable regions of phase space, apart from the line $x = 0$.

Now consider what happens if the phase advance of a cell is a half integer times 2π, so the linear part of the map is just a rotation through π.

If a particle starts at the entrance of a sextupole with $x = x_0$ and $p_x = p_{x0}$, then at the exit of that sextupole:

$$x_1 = x_0, \tag{44}$$

$$p_{x1} = p_{x0} - \frac{1}{2} k_2 L x_0^2. \tag{45}$$

Then, after passing to the entrance of the next sextupole, the co-ordinates will be:

$$x_2 = -x_1 = -x_0, \tag{46}$$

$$p_{x2} = -p_{x1} = -p_{x0} + \frac{1}{2} k_2 L x_0^2. \tag{47}$$

Finally, on passing through the second sextupole:

$$x_3 = x_2 = -x_0, \tag{48}$$

$$p_{x3} = p_{x2} - \frac{1}{2}k_2 L x_2^2 = -p_{x0}. \tag{49}$$

In other words, the momentum kicks from the two sextupoles cancel each other exactly.

The resulting map is a purely linear phase space rotation by π.

In this situation, we expect the motion to be stable (and periodic), no matter what the amplitude.

The effect of the phase advance on the sextupole "kicks" is similar to the effect on perturbations arising from dipole and quadrupole errors in a storage ring.

In the case of dipole errors, the kicks add up if the phase advance is an integer, and cancel if the phase advance is a half integer.

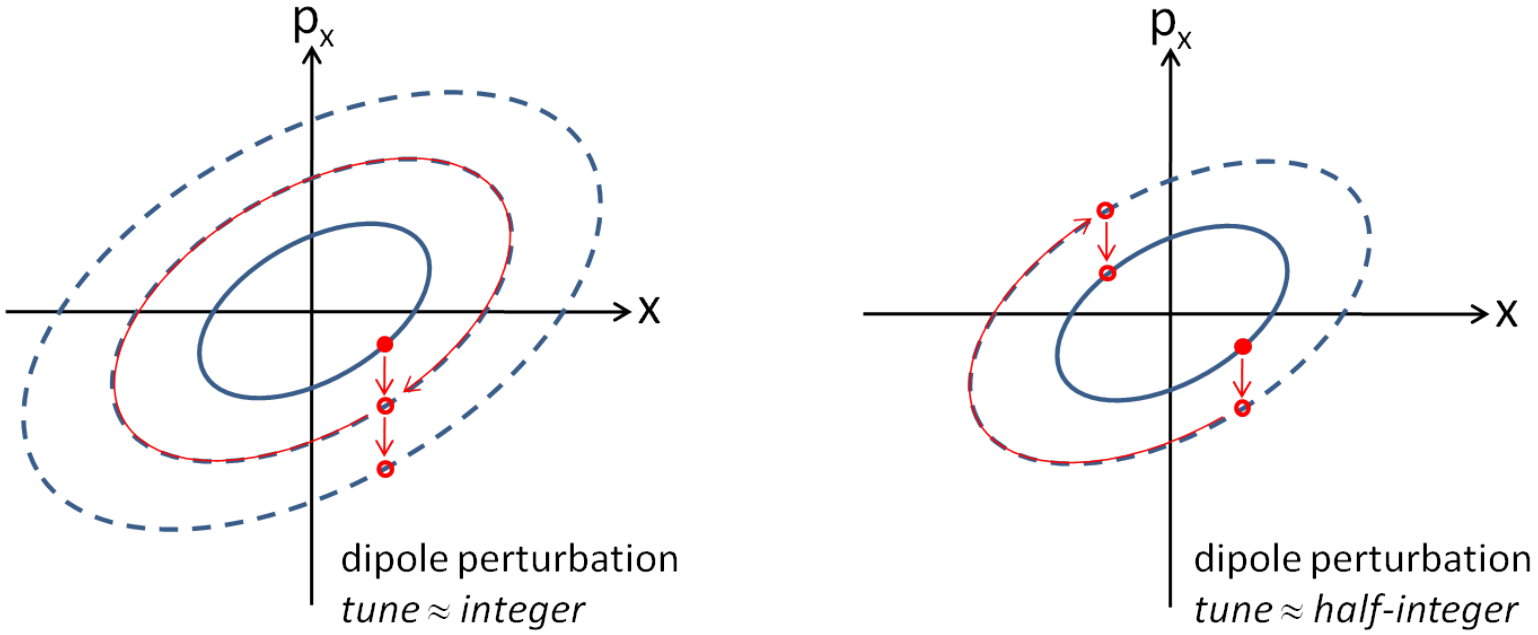

In the case of quadrupole errors, the kicks add up if the phase advance is a half integer.

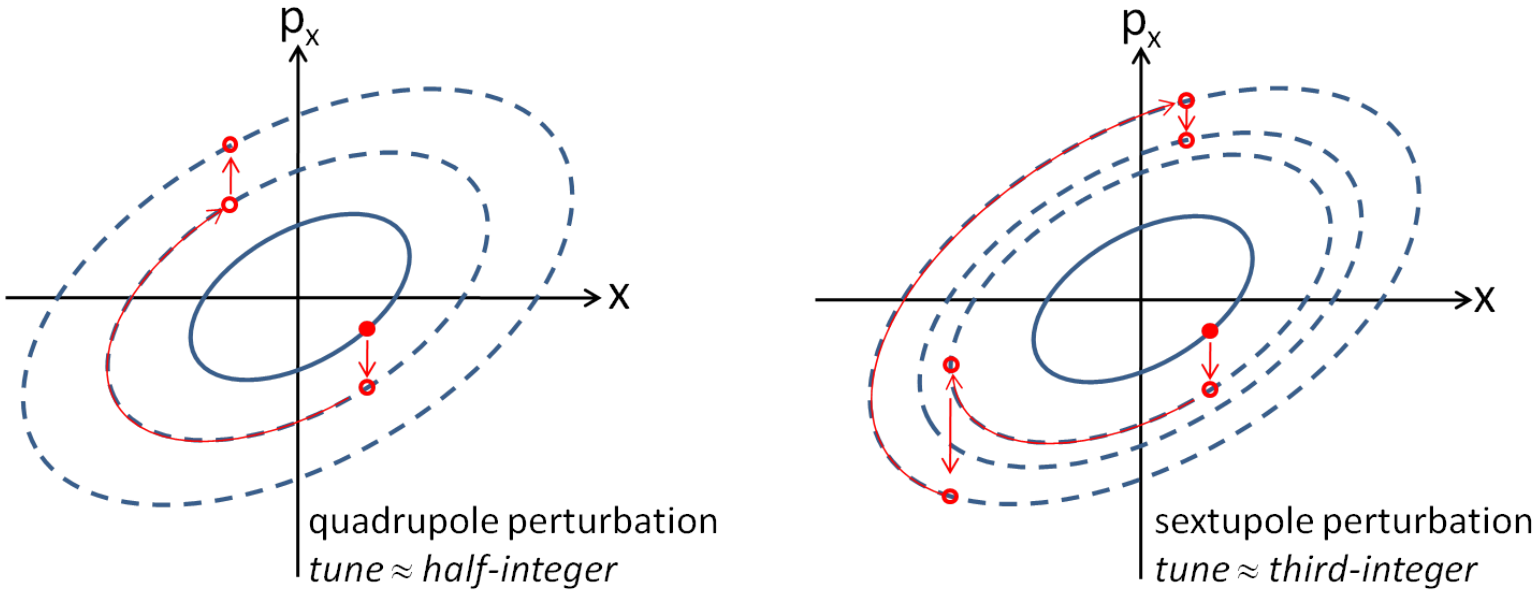

Higher-order multipoles drive higher-order resonances... but the effects are less easily illustrated on a phase space diagram.

If we include vertical as well as horizontal motion, then we find that resonances occur when the tunes satisfy:

$$m_x \nu_x + m_y \nu_y = \ell, \tag{50}$$

where m_x, m_y and ℓ are integers.

The order of the resonance is $|m_x| + |m_y|$.

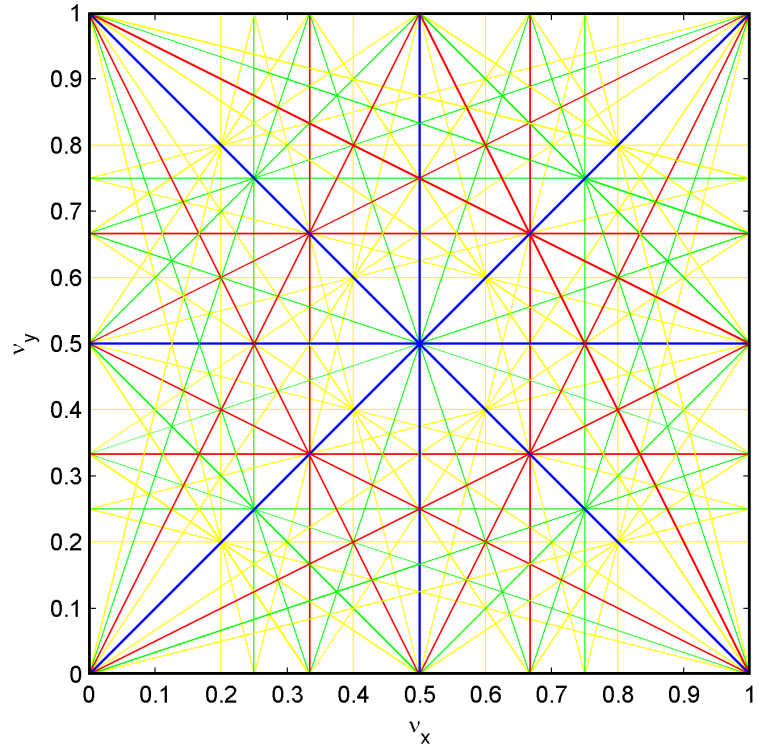

Resonances are associated with unstable motion for particles in storage rings.

However, the number of resonance lines in tune space is infinite: any point in tune space will be close to a resonance of some order.

This observation raises two questions:

1. How do we know what the real effect of any given resonance line will be?
2. How can we design a storage ring to minimise the adverse effects of resonances?

These are not easy questions to answer. We shall discuss some of the issues in the remaining parts of this lecture.

To begin with, for any analysis of nonlinear dynamics we need a convenient way to represent nonlinear transfer maps.

In our analysis of a bunch compressor, we represented the transfer maps for the rf cavity and the chicane as Taylor series.

For example, the longitudinal transfer map for the chicane is:

$$z_1 = z_0 + 2L_1 \left(\frac{1}{\cos\theta_0} - \frac{1}{\cos\theta} \right), \tag{51}$$

$$\delta_1 = \delta_0, \tag{52}$$

where:

$$\theta = \frac{\theta_0}{1+\delta_0}. \tag{53}$$

The map for a chicane can be expanded as a Taylor series:

$$z_1 = z_0 + R_{56}\delta_0 + T_{566}\delta_0^2 + U_{5666}\delta_0^3 + \ldots \quad (54)$$

$$\delta_1 = \delta_0, \quad (55)$$

where the coefficients R_{56}, T_{566}, U_{5666} etc. are all functions of the chicane parameters L_1 and θ_0.

Taylor series provide a convenient way of systematically representing transfer maps for beamline components, or sections of beamline.

The main drawback of Taylor series is that in general, transfer maps can only be represented exactly by series with an infinite number of terms.

In practice, we have to truncate a Taylor map at some order, and we then lose certain desirable properties of the map: in particular, a truncated map will not usually be *symplectic*.

Mathematically, a transfer map is symplectic if it satisfies the condition:

$$J^{\mathsf{T}} S J = S, \tag{56}$$

where $J_{mn} = \partial x_{m,f} / \partial x_{n,i}$ is the Jacobian of the map, and S is the antisymmetric matrix with block diagonals:

$$S_2 = \begin{pmatrix} 0 & 1 \\ -1 & 0 \end{pmatrix}. \tag{57}$$

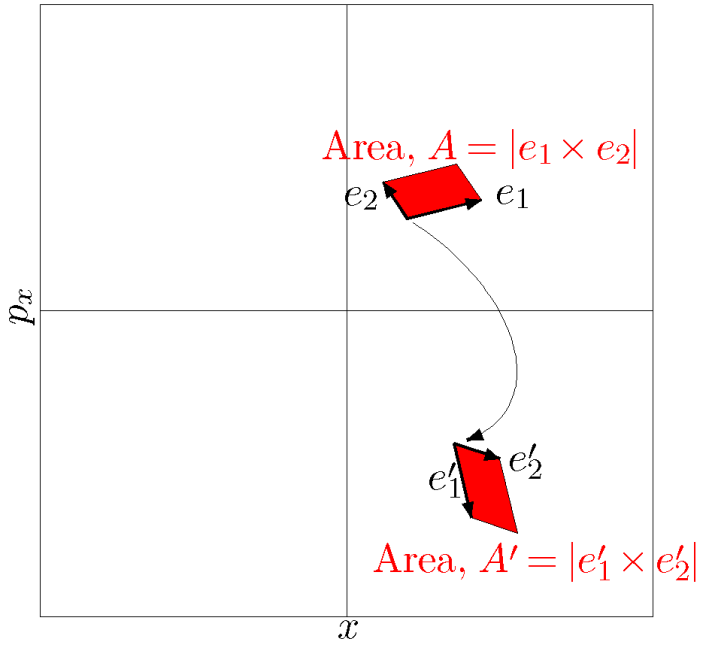

Physically, a symplectic transfer map conserves phase space volumes when the map is applied.

This is Liouville's theorem, and is a property of charged particles moving in electromagnetic fields, in the absence of radiation.

The effect of losing symplecticity becomes apparent if we compare phase space portraits constructed using symplectic (below, left) and non-symplectic (below, right) transfer maps.

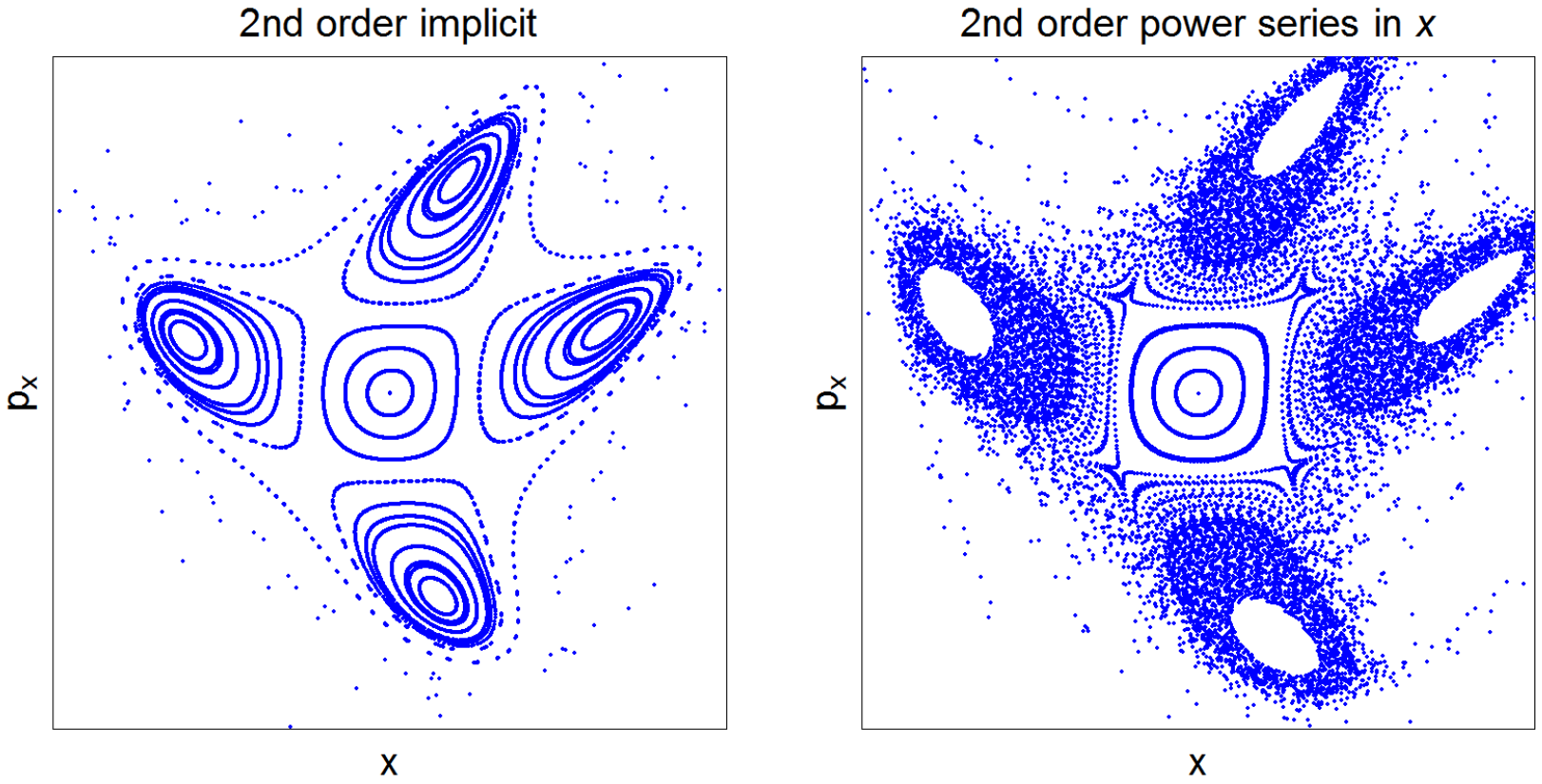

There are a number of ways of representing transfer maps to ensure symplecticity. These include:

- Taylor maps can be specially constructed to retain symplecticity with a certain (finite) number of terms. Taylor maps are *explicit*: once the coefficients have been calculated, the map can be applied simply by substitution of values for the dynamical variables.
- Mixed-variable generating functions provide an *implicit* representation: each application of the map requires further solution of equations (see Appendix B).
- Lie transformations provide a finite representation for infinite Taylor series, and are useful for analytical studies (see Appendix C).

Symplectic Taylor maps with a finite number of terms can be constructed for multipole magnets of any order using the "kick" approximation.

As an example, consider a sextupole, for which the (approximate) equations of motion are:

$$\frac{dx}{ds} = p_x, \qquad \frac{dp_x}{ds} = -\frac{1}{2}k_2 x^2. \tag{58}$$

These equations do not have an exact solution in terms of elementary functions.

However, by splitting the integration into three steps it is possible to write down an approximate solution that is explicit and symplectic:

$$0 \le s < L/2: \qquad x_1 = x_0 + p_{x0}, \quad p_{x1} = p_{x0}, \tag{59}$$

$$s = L/2: \qquad x_2 = x_1, \quad p_{x2} = p_{x1} - \frac{1}{2}k_2 L x_1^2, \tag{60}$$

$$L/2 < s \le L: \qquad x_3 = x_2 + p_{x2}, \quad p_{x3} = p_{x2}. \tag{61}$$

The solution (59)–(60) is an example of a *symplectic integrator*. For obvious reasons, this particular integrator is known as a "drift–kick–drift" approximation.

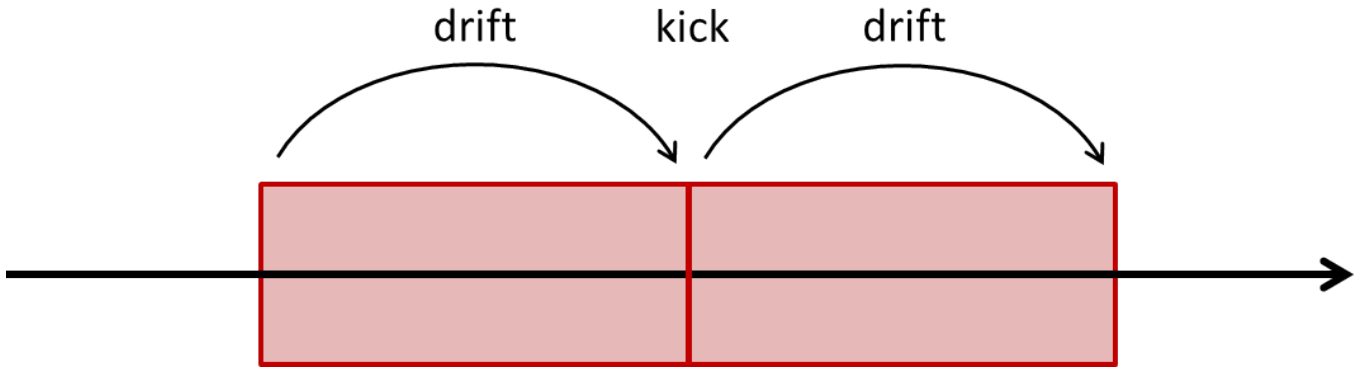

By splitting the integration into smaller steps, it is possible to obtain better approximations.

Using special techniques (e.g. from classical mechanics) it can be shown that by splitting a multipole in particular ways, it is possible to minimise the error for a given number of integration steps.

Taylor maps are useful for particle tracking, but do not give much insight into the dynamics of a given nonlinear system.

To develop a deeper understanding (e.g. to determine the impact of individual resonances) more powerful techniques are needed.

There are two approaches that are quite widely used in accelerator physics:

- perturbation theory;
- normal form analysis.

In both these techniques, the goal is to construct a quantity that is invariant under application of the single-turn transfer map. Unfortunately, in both cases the mathematics is complicated and fairly cumbersome.

In the case of a single sextupole in a storage ring, we find from normal form analysis the following expression for the betatron action J_x as a function of the betatron phase (angle variable):

$$J_x \approx I_0 - \frac{k_2 L}{8}(2\beta_x I_0)^{3/2}\frac{(\cos(3\mu_x/2 + 2\phi_x) + \cos(\mu_x/2))}{\sin(3\mu_x/2)} + O(I_0^2),$$

where I_0 is a constant (an invariant of the motion), ϕ_x is the angle variable, and μ_x is the phase advance per cell.

Note that the second term in the expression for J_x becomes very large when μ_x is close to a third integer.

The cartesian variables can be expressed in terms of the action–angle variables:

$$x = \sqrt{2\beta_x J_x}\cos\phi_x, \tag{62}$$

$$p_x = -\sqrt{\frac{2J_x}{\beta_x}}(\sin\phi_x + \alpha_x\cos\phi_x). \tag{63}$$

Example: normal form analysis of a sextupole in a storage ring

phase advance $\mu_x = 0.28 \times 2\pi$

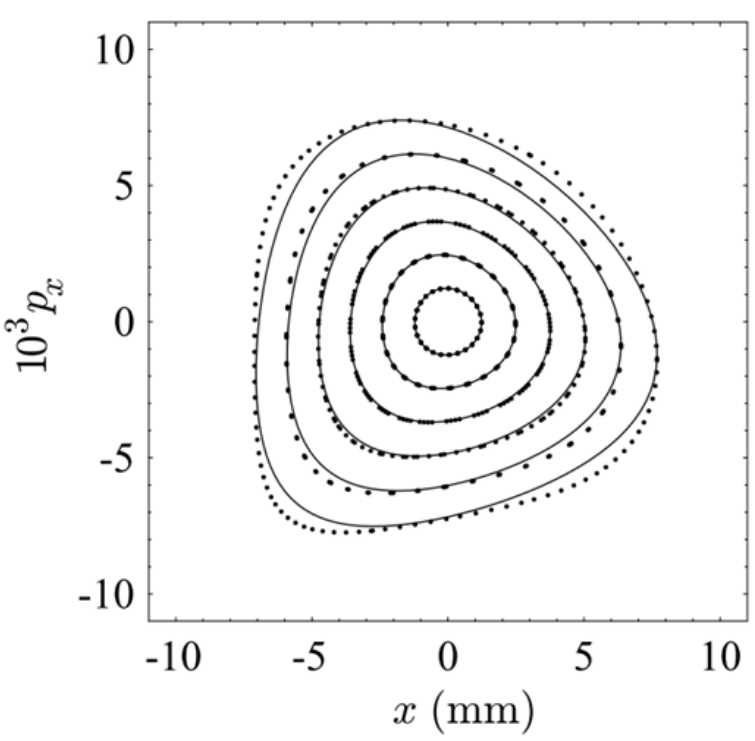

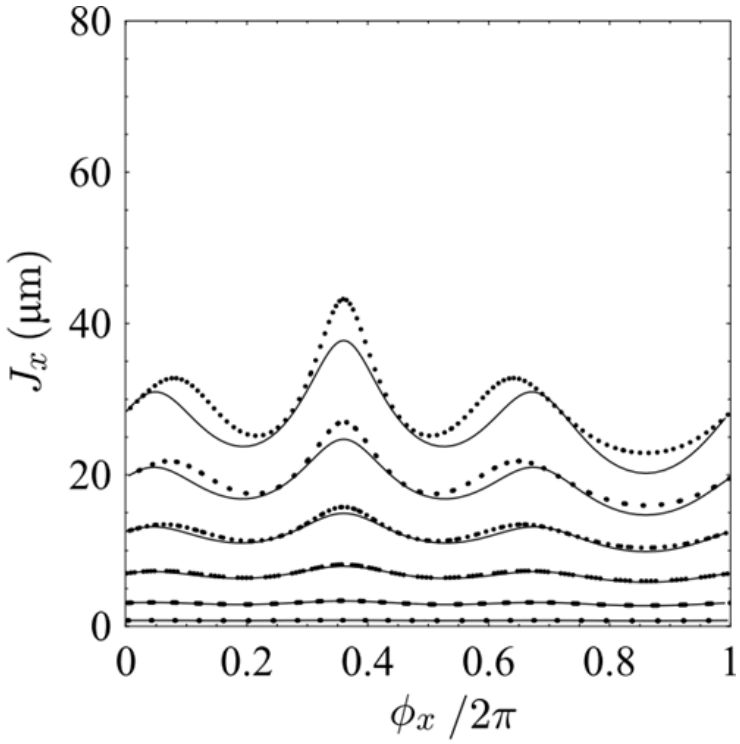

phase advance $\mu_x = 0.30 \times 2\pi$

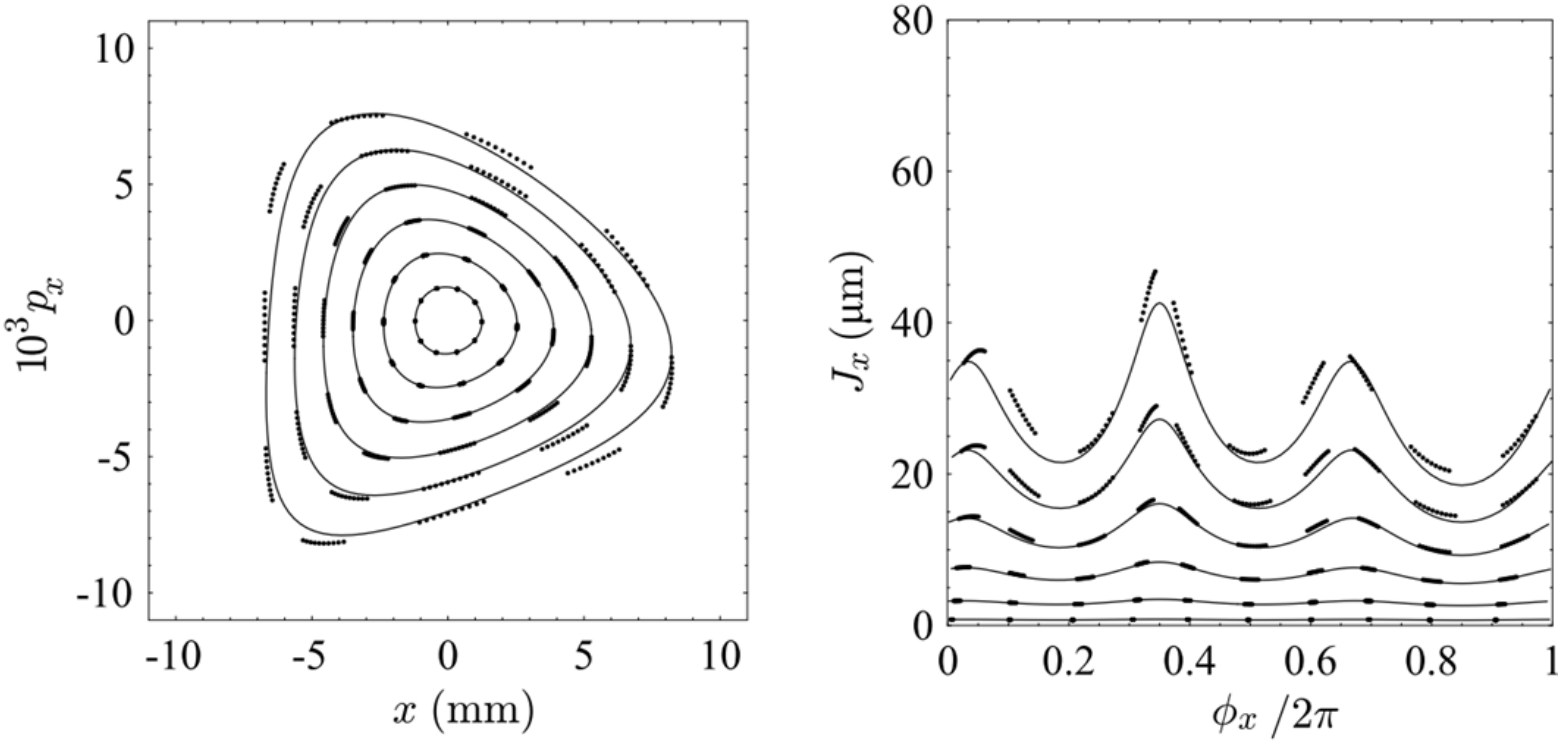

phase advance $\mu_x = 0.315 \times 2\pi$

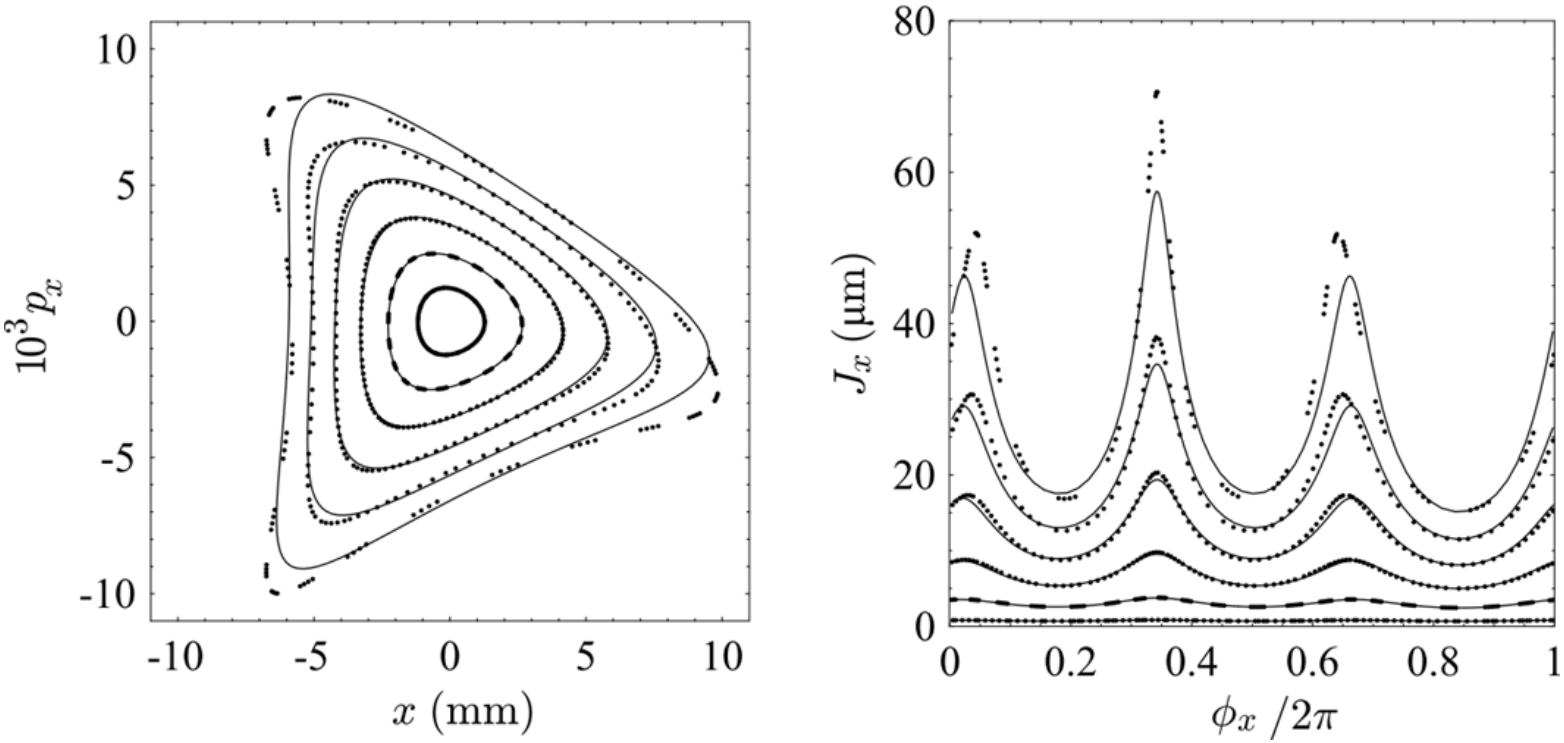

Close inspection of the plots on the previous slides reveals another effect, in addition to the obvious distortion of the phase space ellipses: the phase advance per turn (i.e. the tune) varies with increasing betatron amplitude.

Normal form analysis (and perturbation theory) can be used to obtain estimates for the tune shift with amplitude. In the case of a sextupole, the tune shift is higher-order in the action.

An octupole, however, does have a first-order (in the action) tune shift with amplitude, given by:

$$\nu_x = \nu_{x0} + \frac{k_3 L \beta_x^2}{16\pi} J_x + O(J_x^2). \tag{64}$$

The tune shift with amplitude becomes obvious if we track a small number of turns (30) in a lattice with a single octupole.

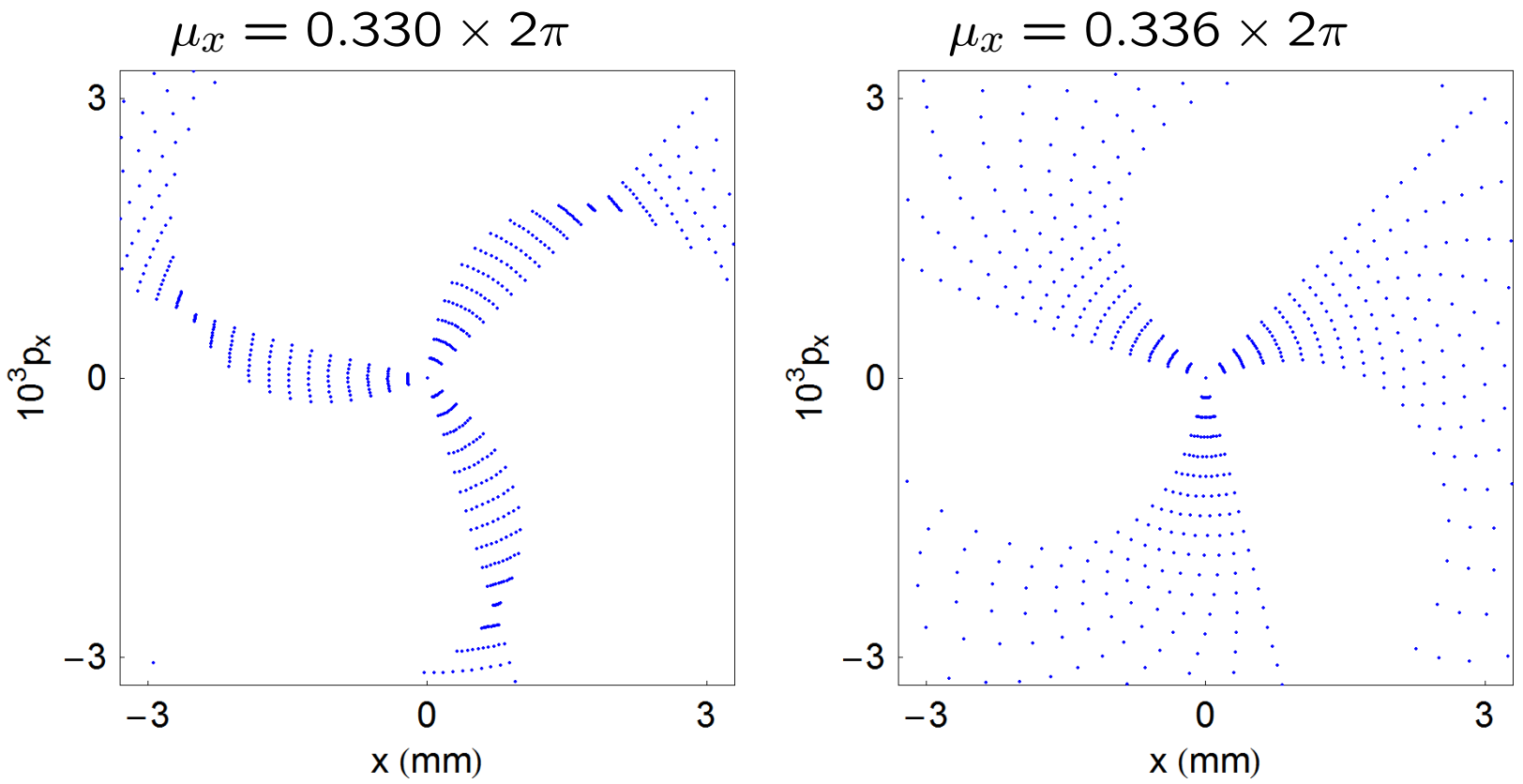

"Islands" appear in phase space portraits at amplitudes where the phase advance is $2\pi\times$ a rational number (that determines the number of islands), and there is a "driving term" (that determines the widths of the islands). Recall the phase space portraits for a sextupole in a storage ring:

$\mu_x = 0.252 \times 2\pi$

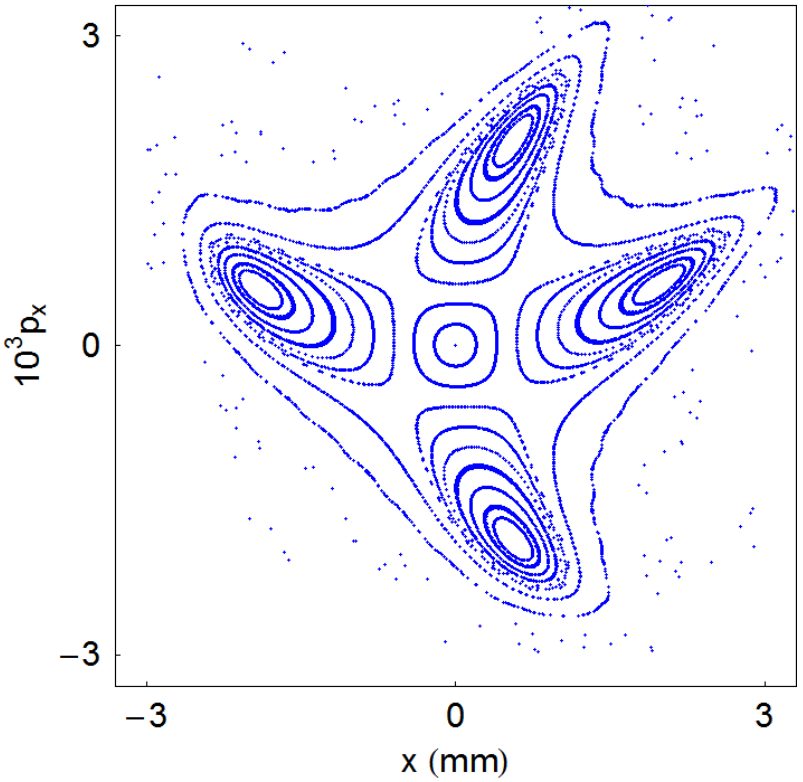

$\mu_x = 0.402 \times 2\pi$

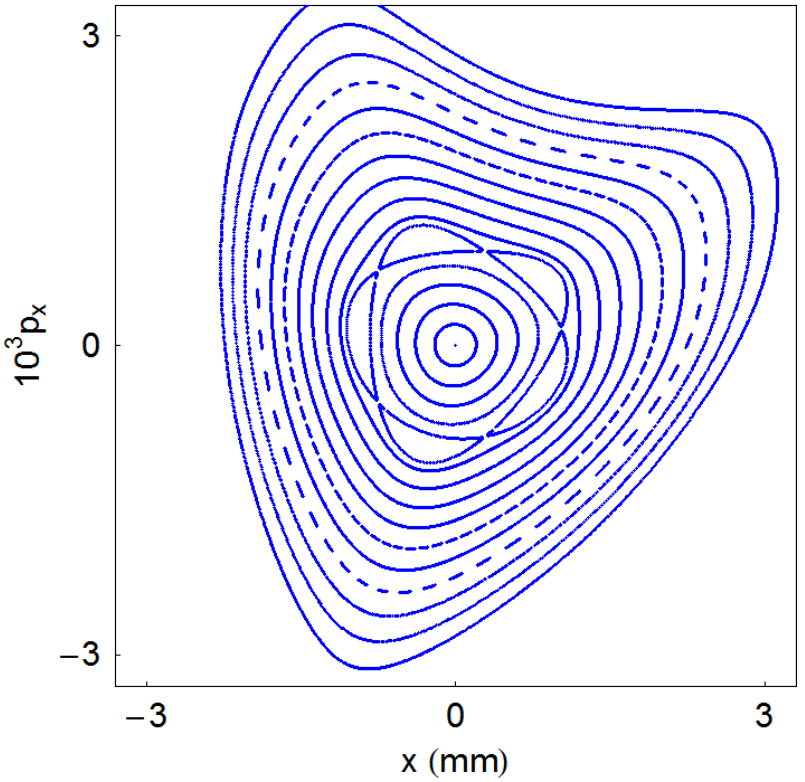

Perturbation theory and normal form analysis depend on the existence of constants of motion in the presence of nonlinear perturbations.

The fact that constants of motion can exist in the presence of nonlinear perturbations is a consequence of the Kolmogorov–Arnold–Moser (KAM) theorem.

The KAM theorem expresses the general conditions for the existence of constants of motion in nonlinear Hamiltonian systems.

Resonances do not invariably result in immediate loss of stability.

In particular, if the tune shift with amplitude is sufficiently large, then it is possible for there to be a stable region at amplitudes significantly larger than that at which resonance occurs.

However, the overlapping of two resonances is associated with a transition from regular to chaotic motion: the parameter range over which the particle motion becomes chaotic is described by the *Chirikov criterion*.

We have shown phase space portraits for motion in one degree of freedom. In those cases, instability occurred when the oscillation amplitude exceeded a certain value.

In multiple degrees of freedom, a new phenomenon occurs: *Arnold diffusion*. There can be regions of phase space where invariant tori exist at large amplitudes compared to regions of chaotic motion.

For storage rings, this means that trajectories with (initially) small amplitudes can be unstable, even if trajectories with much larger amplitudes are stable.

Frequency map analysis and dynamic aperture

Frequency map analysis (FMA) applies "numerical analysis of the Fourier frequencies" to determine the tunes to high precision from tracking data.

The strengths of different resonances can be seen by plotting points in tune space, with diffusion rates shown by different colours.

The boundary of the stable region in co-ordinate space is known as the "dynamic aperture".

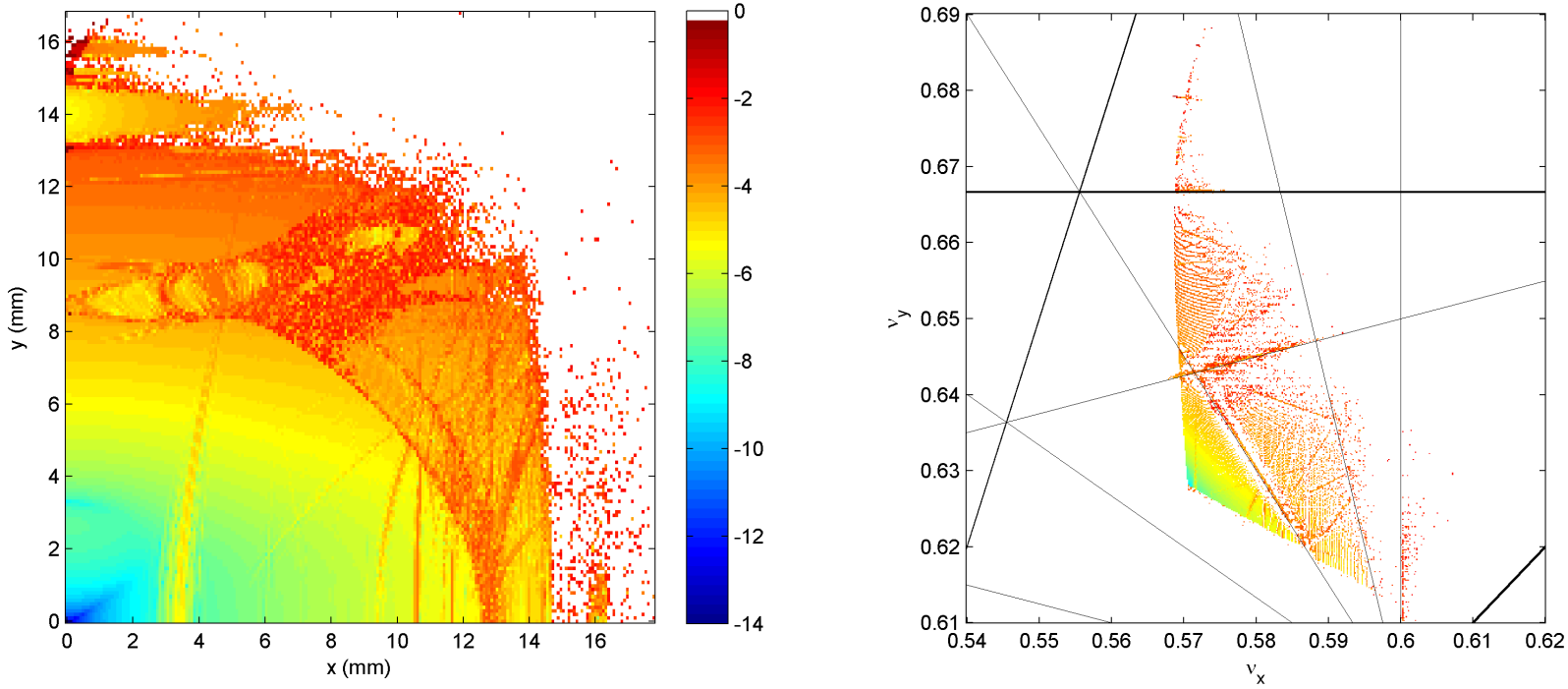

FMA of CesrTA (J. Shanks, Cornell University).

http://www.lepp.cornell.edu/∼shanksj/research/20100629/2048_1024.html

A large dynamic aperture is needed for good injection efficiency, and good lifetime. The dynamic aperture shrinks with energy deviation, limiting the energy acceptance. In low-emittance electron storage rings, beam lifetime is often limited by the dynamic energy acceptance.

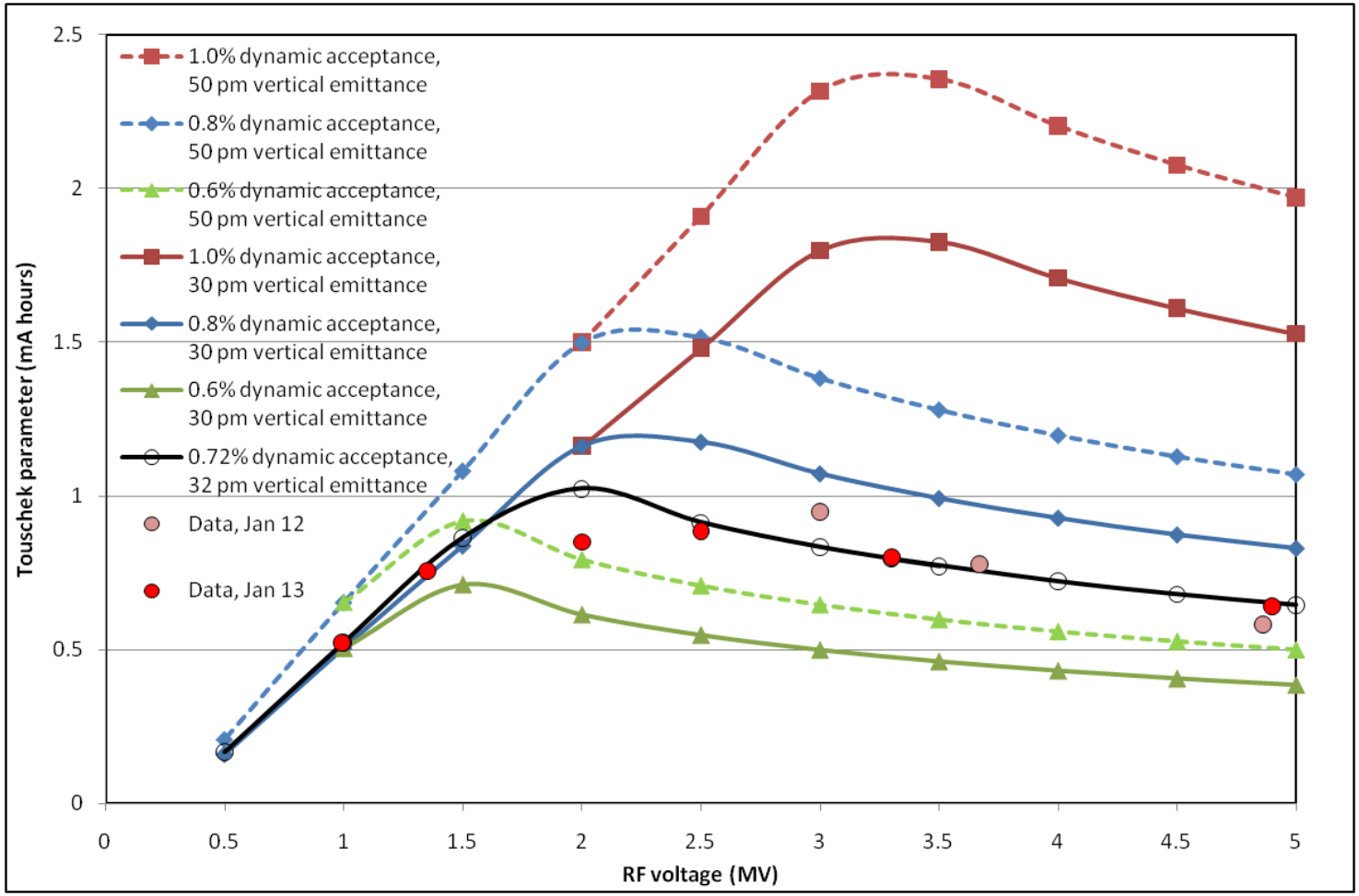

Observation of resonance "islands" in the ALS

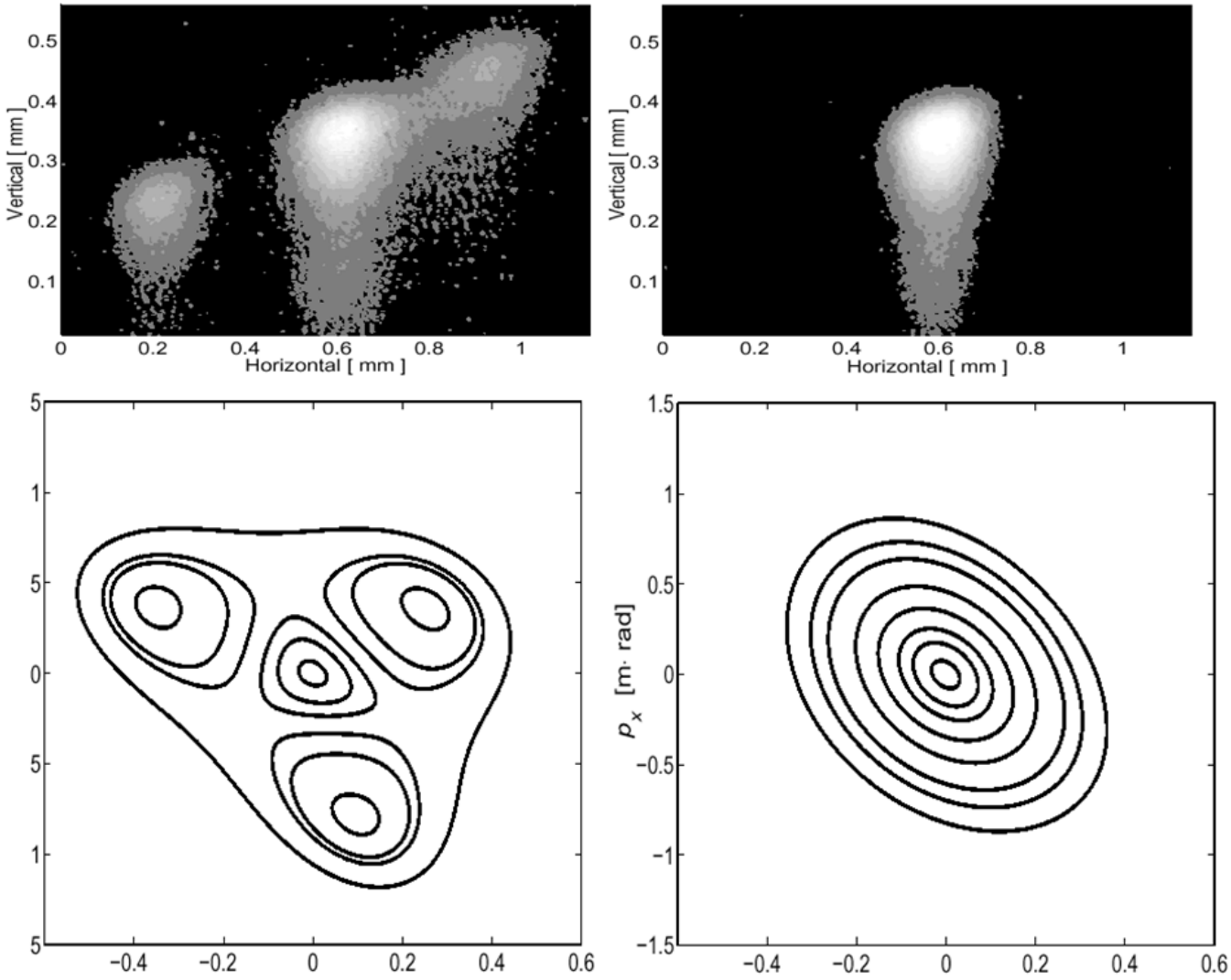

D. Robin, C. Steier, J. Safranek, W. Decking, "Enhanced performance of the ALS through periodicity restoration of the lattice," proc. EPAC 2000.

Summary

Nonlinear dynamics appear in a wide variety of accelerator systems, including single-pass systems (such as bunch compressors) and multi-turn systems (such as storage rings).

It is possible to model nonlinear dynamics in a given component or section of beamline by representing the transfer map as a Taylor series.

Conservation of phase space volumes is an important feature of the beam dynamics in many systems. To conserve phase space volumes, transfer maps must be symplectic.

In general, truncated Taylor maps are not symplectic. There are alternative representations that guarantee symplecticity, but are less convenient (e.g. because they are implicit).

To construct a symplectic transfer map, the equations of motion in a given accelerator component must be solved using a symplectic integrator (e.g. the "drift–kick–drift" approximation for a multipole magnet).

Analytical methods such as perturbation theory and normal form analysis can be used to estimate the impact of nonlinear perturbations in terms of resonance strengths and tune shifts with amplitude.

Frequency map analysis provides a useful numerical tool for characterising tune shifts and resonance strengths from tracking data. This can give some insight into limitations on the dynamic aperture.

H. Goldstein, C.P. Poole Jr., J.L. Safko, *Classical Mechanics* (Pearson, 3rd edition, 2013).

H. Wiedemann, *Particle Accelerator Physics* (Springer, 3rd edition, 2007).

É. Forest, *Beam Dynamics: A New Attitude and Framework* (CRC Press, 1998).

É. Forest, *Geometric integration for particle accelerators*, Journal of Physics A: Mathematical and Theoretical 39, pp. 5321–5377 (2006).

A. Wolski, *Beam Dynamics in High Energy Particle Accelerators* (Imperial College Press, 2014).

Y. Papaphilippou, *Detecting chaos in particle accelerators through the frequency map analysis method*, Chaos: An Interdisciplinary Journal of Nonlinear Science 24, 024412 (2014). doi: 10.1063/1.4884495

Appendices

In a linear approximation, the maps for the rf cavity and the chicane in a bunch compressor may be represented as matrices:

$$M_{\mathrm{rf}} = \begin{pmatrix} 1 & 0 \\ -a & 1 \end{pmatrix}, \qquad M_{\mathrm{ch}} = \begin{pmatrix} 1 & b \\ 0 & 1 \end{pmatrix}, \tag{65}$$

where:

$$a = \frac{eV}{E_0}\frac{\omega}{c}, \quad \text{and} \quad b = 2L_1\frac{\theta_0 \sin\theta_0}{\cos^2\theta_0}. \tag{66}$$

The matrix representing the total map for the bunch compressor, M_{bc}, is then:

$$M_{\mathrm{bc}} = M_{\mathrm{ch}}M_{\mathrm{rf}} = \begin{pmatrix} 1-ab & b \\ -a & 1 \end{pmatrix} = \begin{pmatrix} R_{55} & R_{56} \\ R_{65} & R_{66} \end{pmatrix}. \tag{67}$$

The effect of the map is written:

$$\vec{z} \mapsto M_{\mathrm{bc}}\vec{z}, \quad \text{where} \quad \vec{z} = \begin{pmatrix} z \\ \delta \end{pmatrix}. \tag{68}$$

Now we proceed to derive expressions for the required values of the parameters a and b, in terms of the desired initial and final bunch length and energy spread.

We construct the beam distribution *sigma* matrix by taking the outer product of the phase space vector for each particle, then averaging over all particles in the bunch:

$$\Sigma = \langle \vec{z}\,\vec{z}^{\mathsf{T}} \rangle = \begin{pmatrix} \langle z^2 \rangle & \langle z\delta \rangle \\ \langle z\delta \rangle & \langle \delta^2 \rangle \end{pmatrix}. \tag{69}$$

The transformation of Σ under a linear map represented by a matrix M is given by:

$$\Sigma \mapsto M \cdot \Sigma \cdot M^{\mathsf{T}}. \tag{70}$$

Usually, a bunch compressor is designed so that the correlation $\langle z\delta \rangle = 0$ at the start and end of the compressor. In that case, using (67) for the linear map M, and (70) for the transformation of the sigma matrix, we find that the parameters a and b must satisfy:

$$(1 - ab)\frac{a}{b} = \frac{\langle \delta^2 \rangle_i}{\langle z^2 \rangle_i} \tag{71}$$

where the subscript i indicates that the average is taken over the *initial* values of the dynamical variables.

Given the constraint (71), the compression factor r is given by:

$$r^2 \equiv \frac{\langle z^2 \rangle_f}{\langle z^2 \rangle_i} = 1 - ab, \tag{72}$$

where the subscript f indicates that the average is taken over the final values of the dynamical variables.

We note in passing that the linear part of the map is *symplectic*. A linear map is symplectic if the matrix M representing the map is symplectic, i.e. satisfies:

$$M^{\mathsf{T}} \cdot S \cdot M = S, \tag{73}$$

where, in one degree of freedom (i.e. two dynamical variables), S is the matrix:

$$S = \begin{pmatrix} 0 & 1 \\ -1 & 0 \end{pmatrix}. \tag{74}$$

In more degrees of freedom, S is constructed by repeating the 2×2 matrix above on the block diagonal, as often as necessary.

In one degree of freedom, it is a necessary and sufficient condition for a matrix to be symplectic, that it has unit determinant: but this condition does *not* generalise to more degrees of freedom.

As a specific example, consider a bunch compressor for the International Linear Collider:

Initial rms bunch length	$\sqrt{\langle z^2 \rangle_i}$	6 mm
Initial rms energy spread	$\sqrt{\langle \delta^2 \rangle_i}$	0.15%
Final rms bunch length	$\sqrt{\langle z^2 \rangle_f}$	0.3 mm

Solving equations (71) and (72) with the above values for rms bunch lengths and energy spread, we find:

$$a = 4.9937\,\mathrm{m}^{-1}, \quad \text{and} \quad b = 0.19975\,\mathrm{m}. \tag{75}$$

A mixed-variable generating function represents a transfer map (or, more generally, a canonical transformation) in the form of a function of initial and final values of the phase space variables.

There are different kinds of generating function. A mixed-variable generating function of the third kind is expressed as a function of the initial momenta $\vec{p}$ and final co-ordinates $\vec{X}$:

$$F_3 = F_3(\vec{X}, \vec{p}). \tag{76}$$

The final momenta $\vec{P}$ and initial co-ordinates $\vec{x}$ are obtained by:

$$\vec{x} = -\frac{\partial F_3}{\partial \vec{p}}, \quad \text{and} \quad \vec{P} = -\frac{\partial F_3}{\partial \vec{X}}. \tag{77}$$

As an example, consider the mixed-variable generating function in one degree of freedom:

$$F_3 = -Xp_x + \frac{1}{2}Lp_x^2. \tag{78}$$

Applying (77) leads to the equations:

$$x = X - Lp_x, \quad \text{and} \quad P_x = p_x. \tag{79}$$

In this case, the equations are easily solved to give explicit expressions for X and P_x in terms of x and p_x.

In more general cases, the equations (77) need to be solved numerically each time the transfer map needs to be applied.

Lie transformations make use of the fact that the equations of motion for a particle in an electromagnetic field can be written in the form:

$$\frac{d\vec{x}}{ds} = - :H: \vec{x}, \tag{80}$$

where $\vec{x} = (x, p_x, y, p_y, z, \delta)$ is the phase space vector, and $:H:$ is a Lie (differential) operator:

$$:H: = \sum_{i=1}^{3} \frac{\partial H}{\partial x_i}\frac{\partial}{\partial p_i} - \frac{\partial H}{\partial p_i}\frac{\partial}{\partial x_i}. \tag{81}$$

The precise form of the function $H = H(\vec{x})$ (the Hamiltonian) depends on the field.

Formally, a solution to (80) can be written:

$$\vec{x}|_{s=L} = e^{-L:H:}\, \vec{x}|_{s=0}\,, \tag{82}$$

where the exponential of the Lie operator is defined by its series expansion.

The operator $e^{-L:H:}$ is known as a *Lie transformation*.

Applying a Lie transformation to a phase space variable generally leads to an infinite power series.

However, the power of Lie transformations lies in the fact that:

- there are known mathematical rules for combining and manipulating Lie transformations, and
- for any *generator* $g = g(\vec{x})$ the Lie transformation $e^{:g:}$ represents a symplectic map.